[redacted]

ARDÉ, INC.

GPO PRICE $ _____

CFSTI PRICE(S) $ _____

Hard copy (HC) 3.00

Microfiche (MF) .75

ff 653 July 65

FACILITY FORM 602

N66 37365 (ACCESSION NUMBER)

73 (PAGES)

CR-78165 (NASA CR OR TMX OR AD NUMBER)

(THRU) 1

(CODE) 17

(CATEGORY)

580 WINTERS AVENUE
PARAMUS, NEW JERSEY

FINAL REPORT

FEASIBILITY STUDY OF THE USE OF THERMALLY-INDUCED STRAINING FOR GRAIN REFINEMENT IN RECRYSTALLIZED TUNGSTEN

Contract No. NASw-1145

ARDE, INC. Job No. 4646

Prepared for

NASA-Space Nuclear Propulsion Office

Code NPO, Germantown, Maryland

Prepared by

ARDE, INC.
580 Winters Avenue
Paramus, New Jersey

FEASIBILITY STUDY OF THE USE OF THERMALLY-INDUCED STRAINING FOR GRAIN REFINEMENT IN RECRYSTALLIZED TUNGSTEN

OBJECTIVE

The objective of this program was to demonstrate the feasibility of grain refinement in recrystallized tungsten through thermally induced straining. The ultimate aim was to develop techniques for processing tungsten welds in finished hardware to obtain weld properties similar to those of the base material.

The specific means of achieving these aims are best summarized by the following extract from the Contract Description of Work:

> "Specifically, the Contractor shall design and fabricate or procure 30 simple specimens of recrystallized tungsten which contain a high degree of restraint concentrated in the zone which will be locally heated.
>
> "The Contractor shall induce thermal strain in these specimens using a plasma torch to obtain high heat fluxes at a localized small surface area with time controlled operation. Thermal straining shall be accomplished between the ductile to brittle transition and the recrystallization temperature of the recrystallized tungsten specimens, and the number of straining cycles, cycling rate, heat flux, and heat input will be varied to determine the effect of these variables.
>
> "Post test evaluation of the specimens shall include microhardness measurements, metallographic studies to determine

the effect on grain structure, bend ductility tests to determine the ductile to brittle transition, and X-ray diffraction studies to determine the degree of strain imposed on lattice parameters.

"Based on the results of the above work, the Contractor shall determine the applicability of the thermal straining concept to achieving grain refinement and improved properties in tungsten welds."

SUMMARY AND CONCLUSIONS

The planned program had to be terminated before completion because of inability of Arde's plasma gun to operate continuously without breaking down at the high heat flux necessary to achieve the test objectives. The accomplishments of the program consisted of:

1. Performing the metallurgical studies to set up the required base line data.
2. Accomplishing a number of heating runs to successfully work out the mechanics of fixturing, heating, and instrumentation.
3. Making further calculations to relate the original calculated predictions of cycles to strain more closely to actual heating conditions.
4. Making a number of runs to determine means of elimination of crack formation in specimens.

None of the cycling runs could be sustained to the extent necessary to achieve grain refinement in the tungsten samples. The testing was terminated before a conclusion could be reached as to the validity of the principle of grain refinement by thermal straining. On the other hand, it should be realized that the limited testing accomplished could not be said to disprove the principle. Arde, Inc. is still of the opinion that although assumption limitations in the analysis preclude an exact prediction of cycles to strain, the approach is fundamentally sound and the program was on the right track. It should be possible by the use of a higher powered plasma gun (a number of which are available in other companies) to continue the program to a successful conclusion from its point of termination, while making use of the limited accomplishments of the program as to fixturing, instrumentation, metallurgy and mathematical studies.

BACKGROUND

The development of large nuclear rocket engine components fabricated from refractory metal sheet is hampered by limited sheet sizes plus the inability to satisfactorily join sheet material. The size of tungsten sheets that can be produced is governed by existing size limitations in raw ingot stock and inadequate breakdown facilities for the reduction of preforms. Present maximum sheet width capabilities are 24 inches by General Electric Company in this country, and 36 inches by Metal-Werke Plansee in Austria.

Considerable effort has been expended to produce satisfactory weldments -- especially in tungsten. The fusion techniques investigated include electron beam, atomic hydrogen, heliarc, and conventional electric spot welding. Each of these, unfortunately, results in melted metal with concomitant coarse grain structure, low strength, and brittle weld zones. The greater the heat-affected zone produced, the more brittle and glass-like are the joints. Crack-free welds have been achieved in joints produced by the electron-beam process. Evaluation of electron-beam-welded tungsten coupons shows that maximum strength and ductility are associated with minimum fusion and heat-affected zones, in combination with minimum grain size and smooth continuous weld beads. Even the best welds so produced only develop approximately one-half the strength of the parent metal and have practically no ductility.

Other joining methods in which limited success has been demonstrated are gas-diffusion bonding and brazing. The diffusion-bonding process employs isostatic gas pressure on the order of 10,000 pounds per

square inch, a temperature of 2700°F, and a 3-hour diffusion cycle. Present equipment is limited to 5-inch-diameter specimens -- hence, hardly applicable for full-scale components. The brazing method utilizes a joint cement of nickel or palladium, which is subsequently dispelled through vaporization at low pressures. Joints produced in this manner have been limited to less than 5,000°F capability due to reduced melting temperatures in the joint proper.

It appears likely that sheet size limitations can be overcome by welding followed by hot mechanical working of the weldment to refine the fusion-zone grain structures. Cast and powder metallurgy billets are conventionally hot-worked by rolling, forging, swaging, etc., to develop desired properties. These techniques, of course, cannot be applied to weldments produced in finished components because of the intricate configurations. The required energy for grain refinement can, however, be imparted to welds in complex, finished tungsten hardware, by thermal straining.

The thermal straining concept consists of working welds or cast materials to achieve grain refinement and improved properties by the use of thermal strain. The tungsten would be strained by heating and cooling with the temperature range between its ductile-brittle transition temperature and its recrystallization temperature. This procedure ensures that the tungsten will be ductile and can therefore accommodate a relatively large number of thermal cycles. Calculations contained in Appendix A indicated that the thermal-straining concept appeared feasible.

SPECIMEN DESIGN

Thermal calculations were made to determine the specimen geometry required for achieving the maximum restraint in all directions. For specimen simplicity the study was made on the basis of the desirability of elimination of mechanical restraints imposed through external fixtures. To achieve maximum restraint in all directions by considering material mass surrounding the locally heated area in conjunction with high heat fluxes, sufficient material was needed to allow heat to diffuse in a spherical pattern. This can be accomplished by using a cylinder with a diameter to thickness ratio of two and heating it at the center of the flat face. In order that heat should enter only a small portion of this surface, the flame diameter should be 1/4 of the specimen diameter.

It was decided that those areas on the specimen face which were not to be exposed to direct flame impingement would be thermally shielded to insure that heat entered only through a well defined portion of the specimen surface.

MATERIAL REFERENCE DATA

Unrecrystallized

Tungsten stock in solid cylindrical, unrecrystallized form was procured to serve as a basis for comparing recrystallized thermally strained material as regards microstructural characteristics, hardness, etc. The grain structure of this material, typical of the powder metallurgy consolidation technique of pressing and sintering followed by hot working is shown in Figure 1. A photomicrograph at lower magnification (Figure 2) shows the penetrations made by taking microhardness readings in this material. Indentations were made with a Vickers indentor at a 5 kilogram load and measured at 20 magnifications. The hardness readings converted to Rockwell C values indicate a uniform hardness of R_C 45.0-45.5.

Recrystallized

Typical recrystallized tungsten microstructural characteristics, hardness, etc., prior to undergoing thermal straining are shown in Figures 3 and 4 . The grain structure of the material, typical of recrystallized tungsten is shown in Figure 3. A photo-micrograph at lower magnification (Figure 4) shows the penetrations made by taking micro-hardness readings. Indentations were made with a Vickers indentor at a 5Kg load and measured at 20 magnifications. The hardness readings indicate uniform Rockwell C readings of 38 to 40.

During the course of pulsing portion of the program, the various thermally strained recrystallized samples were to be subjected to photo-micrograph and hardness evaluations. Comparisons with basic recrystallized and non-recrystallized tungsten data were to be made to ascertain the degree of hot working imposed on the recrystallized structure by the controlled operation of the plasma torch.

TEST PARAMETERS

Calculations indicated that in order to thermally work tungsten without mechanical restraints, it would be necessary to achieve a steep temperature gradient. This would be obtained by a high heat flux which would off-set the trend, due to tungsten high thermal diffusivity, toward shallow temperature gradients.

Data taken from previous torch calibration tests indicated that operation with helium as the plasma forming gas would result in a flame energy of 18.4 BTU's per second. Operating conditions to obtain this order of heat flux and an approximate flame temperature of 25,000°F are:

Helium Gas Flow	-	200 S.C.F.H.
Amperage	-	600 Amps
Arc Voltage	-	54 Volts

Test No. 1

A trial test utilizing a tungsten sample was prepared. The intent was to make practice runs on available tungsten prior to receipt of the material on order. By conducting such trial tests, the following was to be established:

1. Torch to sample distance.
2. Method and placement of temperature instrumentation.
3. Cycle time duration and accurate measurement thereof.
4. Correlate flame energy with energy transmitted to sample piece.

Plasma torch operation at a power input of 32.4 kilowatts was conducted to establish the closest practical torch to specimen stand-off distance. A short stand-off distance without damage to the torch face was thought to be desirable because inspiration of ambient air to dilute flame temperature was thereby minimized. Trial runs were conducted at distances down to 1/2 inch without deleterious effects to the plasma torch components. This stand-off distance also appeared to allow sufficient space for a heat shield on the front face of the specimen.

As illustrated in Figures 5, 6, and 7, a half section specimen was used to conduct the trial test. Chromel-alumel thermocouples were used to measure and record both front-face and back side temperatures during the run. A heat shield made from pyrolytic graphite was used to confine the area of direct flame impingement.

The preliminary test run, in which the half section (Figure 8) was used, pointed out the following:

1. The flow of hot gas through the gap between the sample and the pyrolytic graphite base caused an ambient temperature of about 500°F through convective heating.

2. The epoxy resin used to bond the heat shield to the base failed in a matter of seconds causing loss of the shield and full front face heating beyond the target area. Heat penetrated to the resin by radial conduction along the high conductivity plane of the pyrolytic graphite.

Test No. 2

Based on Test No. 1, a new heat shield arrangement was designed (Figure 9). This holding box was made of HLM 85 graphite to afford full protection for full sized specimens. The design attempted to minimize heat conduction from specimen to the holder by maintaining only a four point contact area.

The new heat shield arrangement (Figure 9) was fabricated and tested. Helium plasma torch operation was at 29.8 KW with a stand-off distance of 1/2" based on initial trial tests. Figures 10 , 11, and 12 present various photographs of the sample and heat shield prior to firing. Figures 13 and 14 show the sample and heat shield after firing.

The test indicated that the redesigned heat shield seemed to be adequate for the ensuing thermal pulse tests. For this test, a press fit between the specimen and the box was used to serve the function of a spring load. Examination of the heat shield and sample (Figure 14) after firing indicated only a minimal amount of gas flow between the box and the specimen adjacent to the target area. However, the graphite box cracked (see Figures 13 and 14) due to the thermal expansion of the tungsten, thus requiring a new heat shield for the future tests. The graphite erosion was minimal and the box appeared to be capable of use for repeated firings.

Test No. 3

This test was planned to use a loose fit and a spring load to eliminate the previous expansion problem. Instead of the previous

rotational feed, a side feed arrangement was used. This promised the advantage that before the specimen was fed into the flame, it would be located in a region thermally unaffected by the flame. This was verified during the test, when, with the gun at full power, both thermocouples remained at ambient conditions.

Figure 15 presents the thermocouple temperature history of the cold and hot-sides during firing and soak periods. The cold-side thermocouple, T2, Figure 15, appeared to have lost contact with the specimen at about 500°F, the approximate brittle to ductile transition region of tungsten indicating that the next test, both thermocouples should be spring loaded. The cold-side temperature took approximately four minutes from the beginning of the firing cycle to cool to about 540°F.

The hot-side thermocouple, T1, functioned well up until about 2250°F, after which the readings are in doubt (Figure 15). The thermocouple was lost at 2480°F, a duration of 15 seconds. At 12 seconds, the hot-side thermocouple read 2210°F. Based upon this condition, it was estimated from a thermal analysis of a spherical shell that the cold-side thermocouple should read about 1260°F. The actual reading was 620°F. The extrapolated curve reading is 1000°F, which is reasonable since the thermal analysis neglected the cooling effects of the specimen's cold-side corners.

In summary, these tests substantiated the feasibility of the test rig and ability of helium plasma in order to achieve a reasonable hot-side to cold-side temperature difference.

Tests No. 3 and No. 4

The two tests utilized a loosely fitted tungsten sample in a graphite holder (heat shield). The entire assembly was then spring loaded to minimize cracking of the heat shield. Two views of the test set-up, prior to firing, are shown in Figure 16..

The recrystallized tungsten specimens were loosely fitted in the graphite box to allow for radial thermal growth of the tungsten. Examination of the box and sample after each test indicated only a minimal amount of gas flow between the box and sample adjacent to the target area. During both tests, both graphite holding boxes cracked due to thermal shock as they were moved into the plasma flame. This crack apparently had no thermal effect on the test. After each test, the graphite erosion at the target area was observed to be minimal and the box was capable of withstanding repeated firings.

Tables II, III and IV present a sample test monitoring sheet and two filled-out sheets for Test 3 and 4 respectively.

The two tests were conducted as follows:

Helium plasma torch @ 28.5 KW; stand-off distance of 1/2 inch; peak hot side firing temperature of approximately 2000°F; minimum back-side refire temperature of approximately 500°F; and 45 firing pulses. Test No. 3 utilized argon gas during the soak period to minimize time between firing pulses, whereas Test No. 4 utilized no coolant flow during the soak period. Figure 17 presents postfiring photographs of the two recrystallized samples.

The two samples fired cracked during the tests, however, the pulsing was continued since the depth and severity of the crack would not be determined until the samples were removed from the test rig and examined thoroughly. Since the first recrystallized sample utilized argon as a coolant during the soak period, it was felt that this might be the reason for the cracking. Thus, in Test No. 4 the recrystallized sample was allowed to cool down to 500°F via free convection only. However, the cracking was not eliminated. Visual examination of the exposed gas side tungsten surface after each firing pulse was made for both configurations.

Examination of Tables III and IV indicates that cracking became discernible on or about the fourth cycle for both samples. It is thought unlikely that this was due to thermal fatigue, however, it was decided to review this more thoroughly during the next period. The most probable cause of this cracking was assumed to be thermal shock imposed on the sample during the first heating pulse. It was decided to pursue this aspect of material failure both analytically and experimentally.

Figures 18 and 19 present microstructural characteristics of recrystallized tungsten tests No. 3 and No. 4 after 45 firing pulses. These microstructures are essentially the same as the "as received recrystallized samples" whose characteristics are documented in Figures 3 and 4 . Table I presents Rockwell "C" hardness data obtained from indentations made with a 5 Kg Vickers indentor and measured at 20 magnifications for the datum and fired configurations. In addition, data from a recent Westinghouse Lamp Division Report (WADD-TR-60-37) for refined and recrystallized

tungsten is presented for comparison purposes. Table I indicates a very slight decrease in hardness for the fired configurations. However, this is considered to be within the accuracy of measuring technique. The values documented are average values and were obtained from two microsections per sample (in line and perpendicular (radial) to the plasma gun centerline).

As pointed out previously, since crack severity could not be ascertained until test completion, each sample was subjected to 45 straining cycles, operating between 2000°F and 500°F (Sample 1, Figure 20 and Sample 2, Figure 21). The initial cycle was initiated with the tungsten sample at ambient temperature (Sample 1, Figure 22 and Sample 2, Figure 23), while the subsequent cycles were initiated at approximately 500°F (Sample 1, Figure 24 and Sample 2, Figure 25 and 26). Table V through Table XI present the data ploted in Figures 20 through 26.

Test No. 5

A recrystallized tungsten sample, No. 5, was subjected to a series of runs to evaluate the cracking problem. The object of the first run was to see if thermal shock caused the crack with one firing pulse. Examination under the microscope (30x) indicated no cracking. The sample was run again but this time two firing pulses were used to see if the crack developed on the second pulse with the tungsten specimen starting at approximately 500°F. No cracking was observed. The specimen was rerun for the third time using three firing pulses. Subsequent examination of sample revealed no cracks. The sample was cycled with ten pulses for the last time to determine whether the

crack was formed due to fatigue during the early part of the 45 cycle run of Tests 3 or 4. Microscopic examination revealed no cracks. The sample was cut up after a total of 16 pulses and examined metallurgically. The microstructures showed no apparent change in grain structure while three Vickers indentations (5 Kg load) indicate a Rockwell "C" hardness of approximately 37.

Test No. 6

Since it was not possible to create a crack during Test No. 5, Test No. 6 was set up for a 45 cycle run as a check on crack repeatibility. However, after the sixth pulse the plasma gun developed a water leak in the cooling system and the test had to be terminated. Nevertheless, an examination of sample was made and no cracking was discernable. The gun was dismantled and the fault was found to be a worn "O" ring. It was planned to replace the "O" ring as well as the electrodes which were also worn out. It was tentatively planned that Test No. 7 would be run with the same basic purpose as Test No. 6. However, based on some further calculations which are discussed following, it seemed indicated that the number of pulses might have to be increased appreciably to effect grain refinement. In addition, it was decided that the sample should be preheated to about 500-800°F, the approximate brittle-ductile transition temperature range, prior to pulsing in order to minimize any thermal shock conditions brought about by plasma gun power over-shoot.

Recalculation of Required Cycles to Strain

After Test No. 6, estimates on the degree of thermal strain per cycle for a recrystallized tungsten specimen were made. Ambient (starting) temperature was assumed to vary between 500°F and 1000°F while heating temperature was varied from 1500°F to 2400°F. The analysis was performed utilizing the same simplified approach as described in Appendix A. The number of pulses required to attain an equivalent 50% reduction (mechanical working) was found to increase with increasing ambient temperature and decreasing heating temperature.

The sample was assumed to be completely restrained, Poisson's ratio was neglected and the stress-strain curves for successive pulses were assumed invariant. For the range of Δt's considered, the elastic thermal stresses computed indicate yielding and plastic deformation. The degree of plastic deformation or plastic strain can be found from stress-strain data of recrystallized tungsten. The data for recrystallized tungsten (1 hr. @ 2900°F) was obtained from DMIC Report 127. Figure 27 presents this data for temperatures of 1500, 2000 and 2400°F respectively. The loci of thermal stresses induced in the tungsten for ambient temperature of 500 and 1000°F are also shown in Figure 27 . The intersection of the secant moduli lines with the respective stress-strain curves were obtained from a simple trial and error procedure. Figure 27 shows that percent strain increases with increasing heating temperature and decreasing ambient temperature. Since the sample is theoretically restrained, a compressive strain is induced during heating. On cool-down the compressive strain is relieved and a residual tensile

strain results. If the tensile stress, σ_t, during cool-down is assumed equal to the compressive stress, σ_c, then a first order estimate of the total strain per cycle (heating plus cool-down) can be obtained, i.e. total strain, $\epsilon_{total} = 2\epsilon$. Figure 28 summarizes total strain per cycle and total number of cycles based on an equivalent 50% hot rolling reduction of tungsten. It should be noted here that the total number of pulses required for any combination of test conditions shown in Figure 28 is a minimum value because in reality the tungsten specimen undergoing straining is not fully restrained. The stresses set up during successive heating and cool-down periods will be subject to hysteresis-like effects which will certainly affect total strain per cycle and accumulated total strain. In addition, the stress-strain curves shown in Figure 27 will shift upward during subsequent cycles since the material has been worked, thus requiring greater stresses to achieve a given strain per pulse. Figure 28 can only be utilized for first order estimates and the number of cycles to achieve a predetermined grain refinement will be in excess of the values given in these figures. The samples tested were subjected to 45 cycles using the Helium plasma torch. This is about 10 cycles lower than the predicted minimum (Figure 28). It is obvious that later tests on tungsten samples must be successively pulsed anywhere between 57 and 114 times (i.e. $\epsilon_{total} = 2\epsilon$ and $\epsilon_{total} = \epsilon$) if grain refinement is to be realized.

Test No. 7

As described under Test No. 6 the plasma gun developed a water leak during testing of the sample causing test termination. Upon

disassembly, the "O" rings of water jacket and electrodes were found defective and inoperative and were subsequently replaced. Tungsten Test No. 7 was then installed in the test fixture for its planned 45 cycle excursion. However, this test was also terminated because of excessive plasma gun power overshoot. This power surge (i.e. higher heat flux and temperature) caused a thermal gradient which led to cracking of the sample. Examination of the gun and control console after shutdown did not reveal any discernible cause for the overshoot. It was therefore decided to install another specimen and recheck the reworked plasma gun setup.

Test No. 8

In order to avoid thermal shocking due to the power overshoot condition experienced in Test No. 7, Test No. 8 was preheated to 600°F for 1-1/2 minutes prior to imposing the pulsing cycle. During the 14th cycle, a thin line was observed in the vicinity of hot side drilled hole. The test was subsequently terminated in the 15th cycle when it was definitely established that the specimen had failed. Subsequent examination revealed the crack initiated initiated in the high stress region of the hot side drilled hole and it was decided to eliminate this hole from future pulsing schedules and utilize only the back or so called "cold" side thermocouple.

Test No. 9

The ninth sample was prepared and preheated prior to pulsing. Firing was initiated at 800°F and terminated when backside temperature reached 1100°F. This temperature variation was estimated using the

previous specimen firing temperature histories. However, after the 53rd cycle, the test was terminated because of gun face melting and severe water leaks. The sample was examined and found to be sound, visually and metallurgically. However, little or no change was observed.

Tests No. 7 and No. 8 had brought out several weaknesses in the plasma gun operation and sample preparation techniques. Out of this series of mishaps, a new testing technique was evolved for No. 9. The cold side thermocouple was retained. The elimination of the hot side thermocouple promised alleviation of the high stress region brought about by drilling, while preheating to 800°F prior to pulsing promised to assure that the sample would be well above its brittle-ductile transition temperature. Based on the previous sample temperature histories, the backside temperature during firing required to achieve a hot side ΔT of about 1500°F was estimated to be about 1100°F. This value was subsequently utilized in pulsing Test No. 9.

The analysis made after Test No. 6 indicated that approximately 55-60 cycles would be required to ideally achieve grain refinement for the new testing technique (800°F to 2300°F). However, based on the various assumptions made in this analysis, the actual number of pulses planned to be imposed on specimen No. 9 was doubled (i.e. 120 cycles).

As pointed previously, recrystallized tungsten Test No. 9 was subjected to 53 straining cycles before the test was terminated due

to the plasma gun developing a water leak as a result of severe gun-face melting. The sample was pre-heated slowly for about three minutes till a back-side temperature of about 860°F was reached by using the plasma gun at one-half power with the plasma flame impinging on the corner of the graphite holding box. The sample was then allowed to cool to a uniform temperature of about 800°F before thermal cycling was begun. Since the hot-side thermocouple (T1) was eliminated, the cold-side thermocouple (T2) was used to monitor the test. A typical thermal cycle starts with the sample at about 800°F and with the gun at full power. The sample is then placed in firing position. When the back-side temperature reaches about 1100°F, the plasma flame is extinguished and the sample is allowed to cool to 800°F (the start of the next cycle). The firing pulse of each cycle was measured by a stop watch and is tabulated in Table XII (shown in Figure 29). The general trend of shorter firing pulses as cycling progresses is consistent with past tests. However, due to the melting of the plasma gun's face, steady-state operation was not achieved. The maximum and minimum cold-side temperatures were recorded, in Table XIII, and are shown in Figure 30 . Except for two points, the operating temperature range was fairly constant. Examination of the specimen under the microscope showed that the sample was sound (i.e. no cracking).

The sample was cut up in several planes and metallurgically examined. Grain structure appeared to be unchanged from that of the datum re-crystallized tungsten sample, while average Rockwell "C" hardness were comparable to the non-pulsed recrystallized tungsten specimen.

APPENDIX "A"

1. ESTIMATE OF THERMAL STRAIN PER CYCLE AND NUMBER OF CYCLES REQUIRED FOR THERMAL STRAINING

Consider a flat tungsten sheet that is heated locally. If we assume 100% restraint and neglect Poisson"s ratio effects, the elastic thermal stress, σ may be approximated by:

$$\sigma = E \alpha \Delta T \qquad (1)$$

For tungsten take

ΔT = temperature change = 2400°F-100 = 2300°F

E = Young's Modulus = 22×10^6 psi (at 2400°F)

α = Coefficient of thermal expansion = 3.3×10^{-6} in/in°F

Then we find from (1),

$$\sigma = (22 \times 10^6)\ (3.3 \times 10^{-6})\ (2300°F) = 167{,}000 \text{ psi}$$

which indicates yielding and plastic deformation. To estimate the plastic strain, we employ Figure 31 , which gives stress-strain curves of tungsten as a function of temperature, reference 3 .

Assuming a secant modulus of 1.95×10^6 psi at 2400°F, the thermal stress becomes,

$$\sigma = (\alpha_{\text{secant}})\ \Delta T = 1.95 \times 10^6 \times 3.3 \times 10^{-6} \times 2300°F = 14{,}800 \text{ psi}$$

and from Figure 31, the corresponding strain is .0075 in/in. This is a compressive strain induced by heating to 2400°F. As the local-

ized heated area cools, the induced compressive strain is relieved and a residual tensile strain results. Assuming the residual tensile strain is essentially equal to the compressive strain, or .0075 in/in., we estimate the order of the total plastic strain due to heating and cooling as .015 in/in.

To obtain a textured grain with concomitant property improvement by hot working of tungsten, reduction by hot rolling on the order of 50% is conventional. This implies 33 thermal cycles at 1-1/2% strain per cycle to achieve straining by thermal means comparable to that obtained by mechanical working.

2. THERMAL FATIGUE CONSIDERATIONS

To estimate the cycles to failure by thermal fatigue, we use the results of references 1, 2.

$$N_f^{\,k} \epsilon_p = C \qquad (2)$$

and take for tungsten

$$k = 1/2$$

$$\epsilon_p = .015 \text{ in/in.}$$

$$C \cong \epsilon_f = \text{true static tension fracture strain} \cong 0.75 \text{ in/in.}$$

which yields from (2) the cycles to failure,

$$N_f = (\epsilon_f/\epsilon_p)^2 = (.75/.015)^2 = 2500 \text{ cycles}$$

Since $N_f >> 33$ cycles, we conclude that thermal fatigue is not likely.

3. THERMAL SHOCK CONSIDERATIONS

Thermal shock possibilities may be minimized or eliminated by operating between the ductile - brittle transition temperature and the recrystallization temperature (about 400°F to 2500°F). The tungsten would then be ductile and the discussion of section 2 above would apply.

REFERENCES

(1) Manson, S. S. "Behavior of Materials Under Conditions of Thermal Stress", TN 2933, NACA 1953.

(2) Coffin, L. F. Jr., "A Study of the Effects of Cyclic Thermal Stresses on a Ductile Metal", Trans. ASME, Vol. 76, 1954, p. 923.

(3) DMIC Report 127, March 15, 1960, Battelle Memorial Institute.

ARDE, INC.

HARDNESS COMPARISONS

CONFIGURATION	AVERAGE ROCKWELL "C" READINGS
1. As Swaged (Un-recrystallized, As Received) - Datum	45.3 *
2. Recrystallized (As Received) - Datum	38.2 *
3. Recrystallized Sample No. 1 (45 Pulses) (Test No. 3)	35.8 *
4. Recrystallized Sample No. 2 (45 Pulses) (Test No. 4)	37.3 *
5. Comparisons from Data in WADD-TR-60-37-Part V - August 1964	
a) As Swaged	~45.5
b) Annealed @ 1832°F	~45.6
c) Annealed @ 2190°F	~44.2
d) Annealed @ 2555°F	~38.2
e) Annealed @ 2730°F	~38.2

* Indentations - Vickers Indentor @ 5 Kg load & measured @ 20 magnifications

TABLE I

PLASMA OPERATIONAL SHEET

Console and Rectifier	Remarks
1. Open Circuit Voltage	
2. Gun Type	
3. Arc Gas Flowmeter	
4. Arc Gas S.C.F.H.	
5. Power Control Start	
6. Amps	
7. Volts	
8. K.W.	
9. Electrode Front	
10. Electrode Rear	

Hopper	
1. Powder Type and Mesh	
2. Carrier Gas	
3. Carrier Gas Flowmeter	
4. Carrier Gas S.C.F.H.	
5. Hopper Venturi Setting	

Cooling Circuit	
1. Water Temp. In	
2. Water Temp. Out	
3. Water Flow G.P.M.	

Auxiliary Equipment	
1. Gas Bottle Regulator Press.	
2. Spraying Environment	
3. Chamber Pressure	

TABLE II

6/3/65

Recrystallized Tungsten Sample #1 (Test #3) Thermo-Straining 4642.

PLASMA OPERATIONAL SHEET

Console and Rectifier

1. Open Circuit Voltage 160 V.
2. Gun Type F-40
3. Arc Gas Flowmeter 2.8 on H_2
4. Arc Gas S.C.F.H. 200 SCFH He
5. Power Control Start —
6. Amps 600
7. Volts 47½
8. K.W. 28.5
9. Electrode Front Standard
10. Electrode Rear

Hopper

1. Powder Type and Mesh
2. Carrier Gas
3. Carrier Gas Flowmeter
4. Carrier Gas S.C.F.H.
5. Hopper Venturi Setting

} None

Cooling Circuit

1. Water Temp. In 58° F
2. Water Temp. Out 66° F
3. Water Flow G.P.M. 3.6 G.P.M.

Auxiliary Equipment

1. Gas Bottle Regulator Press. 50
2. Spraying Environment open air
3. Chamber Pressure —

Remarks

Helium on Hydrogen flowmeter.

Helium bottle pressure when starting 1400 p.s.i.G.
Stop: 500 p.s.i.G. = 900 p.s.i.G. mixed

Argon for cooling:
start - 2000 p.s.i.G.
STOP - 1300 " " "
USED - 700 " " "
Amount of Cycle

Start 2³⁰ P.M.

5 10 15 20 25
30 35 40 45 = 45 cycles

Stop: 4³⁰ P.M.

Gun on approximately 5 secs at full power.

* Specimen shows "Crack" (5th Cycle)

TABLE III

6/7/65

RECRYSTALLIZED TUNGSTEN #2 Job #4646

M. Stringas

T. Lerma - attaining

PLASMA OPERATIONAL SHEET

(TEST #4)

Console and Rectifier

1. Open Circuit Voltage 160
2. Gun Type F-40
3. Arc Gas Flowmeter 2.8 Helium
4. Arc Gas S.C.F.H. 200
5. Power Control Start 10
6. Amps 600
7. Volts 47.5
8. K.W. 28.5
9. Electrode Front } Standard
10. Electrode Rear }

Hopper

1. Powder Type and Mesh
2. Carrier Gas
3. Carrier Gas Flowmeter
4. Carrier Gas S.C.F.H.
5. Hopper Venturi Setting

} None

Cooling Circuit

1. Water Temp. In 72°F
2. Water Temp. Out 78°F
3. Water Flow G.P.M. 3.5

Auxiliary Equipment

1. Gas Bottle Regulator Press. 50
2. Spraying Environment open air
3. Chamber Pressure not used

TABLE IV

Remarks

Helium bottle pressure
Start - 1375 P.S.I.G.
Stop - 575
95

Cycling Time
6/7/65
Start - 10:03 AM
Stop - 1:20 P.M

Amount of cycles

5 10 15 20 25
30* 35* 40** 45

Chart paper ran out on 44th cycle. (Back thermo-c'pl.)

* A "line" or possible "crack" appeared after 4th cycle.
* - "possible crack" at 8 cycle
* appears to be line from 2 o'clock to 10 on cycle # 13
* Crack at 9 o'clock from backside noticed cycle 14
* observed crack from 3 o'clock

TABLE V - THERMOCOUPLE TEMPERATURE HISTORY

Sample 1 (Test #3)

Cycle 1

t ~ Sec.	T1 ~ °F	T2 ~ °F	t ~ Sec.	T1 ~ °F	T2 ~ °F
0	70	55			
1	310	55	21	1300	1045
2	570	60	22	1285	1045
3	755	142	23	1270	1045
4	942	197	24	1258	1042
5	1065	260	25	1242	1038
6	1232	345	26	1230	1028
7	1383	425	27	1218	1018
8	1540	512	28	1205	1010
9	1700	610	29	1195	1005
10	1850	718	30	1182	1000
11	2000	825	40	1084	928
11.5	2070	880	50	1000	860
12	1862	930	60	927	810
13	1620	1020	70	862	750
14	1505	1065	80	818	705
15	1442	1047	90	759	663
16	1400	1045	100	718	624
17	1370	1045	110	679	593
18	1348	1045	120	640	562
19	1330	1045	130	609	520
20	1315	1045	135.3	595	505

TABLE VI - THERMOCOUPLE TEMPERATURE HISTORY

Sample 1 (Test #3)

Cycle 2

t ~ Sec.	T1 ~ °F	T2 ~ °F	t ~ Sec.	T1 ~ °F	T2 ~ °F
0	595	505	23	1280	1092
1	880	505	24	1270	1089
2	1145	518	25	1259	1082
3	1355	550	26	1249	1080
4	1520	600	27	1239	1070
5	1665	660	28	1230	1064
6	1795	725	29	1220	1058
7	1915	810	30	1212	1050
8	2025	900	40	1122	970
9	1705	995	50	1045	904
10	1550	1055	60	980	844
11	1480	1062	70	920	800
12	1432	1064	80	868	753
13	1402	1075	90	824	710
14	1382	1085	100	780	680
15	1363	1090	110	747	650
16	1350	1095	120	712	618
17	1340	1095	130	682	592
18	1329	1095	140	655	570
19	1319	1095	150	629	528
20	1309	1095	153	620	520
21	1300	1095			
22	1290	1092			

ARDE, INC.

TABLE VII - MAXIMUM & MINIMUM THERMOCOUPLE TEMPERATURE PER CYCLE

Sample 1 (Test#3)

CYCLE	T1 ~ °F		T2 ~ °F	
	Max.	Min.	Max.	Min.
0	70	70	55	55
1	2070	595	1065	505
2	2025	620	1095	520
3	2010	580	1080	490
4	1965	580	1050	495
5	2020	595	1050	510
6	2000	595	1060	505
7	2000	620	1030	515
8	1995	600	1040	500
9	1980	610	1015	520
10	1995	620	1030	520
11	2000	620	1015	515
12	2000	620	1020	510
13	2000	605	995	510
14	2000	600	1000	500
15	2005	600	1000	500
16	2005	610	1015	510
17	2030	600	1030	500
18	2000	600	1005	500
19	2000	600	980	505
20	2020	605	1010	510
21	1990	600	990	500
22	2000	600	995	500
23	1995	595	1000	500
24	2020	605	1000	505
25	2000	600	970	510
26	2000	600	1000	500
27	1995	600	1000	500
28	2000	600	970	500
29	2000	600	980	500
30	2000	600	980	505
31	2020	600	995	500
32	2000	600	975	500
33	2000	600	1000	500
34	2020	600	985	500
35	2010	600	990	505
36	2005	600	970	505
37	2005	600	985	505
38	1995	590	975	500
39	2000	600	985	500
40	2010	600	965	510
41	2010	600	970	500
42	1995	600	980	500
43	2010	600	960	505
44	2010	600	965	510
45	2000	70	955	55

TABLE VIII - THERMOCOUPLE TEMPERATURE HISTORY

Sample 2 (Test #4)

Cycle 1

t ~ Sec.	T1 ~ °F	T2 ~ °F	t ~ Sec.	T1 ~ °F	T2 ~ °F
0	75	90	28	1235	1105
1	310	90	29	1225	1100
2	515	108	30	1215	1090
3	720	150			
4	925	215	31	1205	1083
5	1100	287	32	1197	1078
6	1265	365	33	1189	1068
7	1430	455	34	1180	1058
8	1590	550	35	1170	1050
9	1745	645	36	1162	1045
10	1880	745	37	1152	1040
10.8	1995	830	38	1142	1032
11	1950	850	39	1133	1025
12	1640	950	40	1125	1020
13	1500	1025	50	1042	950
14	1420	1015	60	973	890
15	1380	1030	70	910	830
16	1355	1050	80	855	780
17	1340	1070	90	805	737
18	1325	1083	100	763	700
19	1315	1095	110	725	657
20	1305	1103	120	692	632
21	1298	1108	130	662	608
22	1290	1110	140	637	582
23	1280	1110	150	612	552
24	1272	1110	160	600	528
25	1265	1110	164	582	520
26	1252	1110			
27	1245	1110			

TABLE IX - THERMOCOUPLE TEMPERATURE HISTORY

Sample 2 (Test #4)

Cycle 2

t ~ Sec.	T1 ~ °F	T2 ~ °F	t ~ Sec.	T1 ~ °F	T2 ~ °F
0	582	520	26	1252	1138
1	825	520	27	1244	1132
2	1075	530	28	1235	1128
3	1275	567	29	1228	1120
4	1465	617	30	1217	1113
5	1660	680	40	1133	1048
6	1815	765	50	1062	987
7	1965	857	60	1000	930
7.2	1995	875	70	948	882
8	1750	928	80	903	838
9	1575	972	90	862	800
10	1475	1028	100	828	770
11	1425	1069	110	797	740
12	1392	1100	120	770	718
13	1372	1120	130	745	690
14	1359	1132	140	722	670
15	1349	1142	150	702	650
16	1340	1150	160	682	630
17	1332	1152	170	665	618
18	1322	1155	180	648	600
19	1314	1155	190	632	587
20	1305	1155	200	618	570
21	1298	1155	210	603	550
22	1290	1155	220	592	538
23	1280	1152	227.5	582	532
24	1270	1150			
25	1262	1143			

ARDE, INC.

TABLE X - THERMOCOUPLE TEMPERATURE HISTORY

Sample 2 (Test #4)

Cycle 3

t ~ Sec.	T1 ~ °F	T2 ~ °F	t ~ Sec.	T1 ~ °F	T2 ~ °F
0	582	532	28	1215	1115
1	870	532	29	1205	1110
2	1120	540	30	1198	1102
3	1342	575	40	1124	1038
4	1542	635	50	1060	982
5	1722	700	60	1003	930
6	1890	785	70	955	888
6.6	1975	845	80	912	845
7	1850	875	90	875	810
8	1600	920	100	843	780
9	1480	977	110	813	750
10	1410	1028	120	789	730
11	1372	1065	130	762	705
12	1350	1090	140	740	685
13	1335	1110	150	720	665
14	1322	1120	160	700	648
15	1312	1128	170	685	632
16	1305	1132	180	668	620
17	1298	1138	190	652	604
18	1292	1138	200	638	592
19	1283	1138	210	625	575
20	1275	1138	220	612	560
21	1267	1138	230	600	550
22	1259	1138	240	588	538
23	1250	1138	244.3	582	530
24	1244	1135			
25	1237	1130			
26	1230	1125			
27	1222	1120			

ARDE, INC.

TABLE XI - MAXIMUM AND MINIMUM THERMOCOUPLE TEMPERATURES PER CYCLE

Sample 2 (Test #4)

CYCLE	T1 ~ °F		T2 ~ °F	
	Max.	Min.	Max.	Min.
0	75	75	90	90
1	1995	582	1110	520
2	1995	582	1155	532
3	1975	582	1138	530
4	1970	580	1105	530
5	2000	565	1115	525
6	2000	560	1130	510
7	2000	555	1105	510
8	2000	550	1100	500
9	1995	545	1070	500
10	2000	550	1090	500
11	2000	550	1095	500
12	1980	540	1080	500
13	2015	540	1110	495
14	1990	540	1085	500
15	1995	540	1070	500
16	1985	540	1065	495
17	2000	540	1070	500
18	2000	540	1075	500
19	2000	540	1080	495
20	2000	540	1090	500
21	1990	540	1050	500
22	2010	540	1080	500
23	2000	545	1060	500
24	2005	545	1070	500
25	2000	540	1095	500
26	2010	535	1060	500
27	2010	535	1080	500
28	2035	540	1090	500
29	2000	540	1090	500
30	2005	545	1080	500
31	2020	535	1075	500
32	2035	540	1075	500
33	2005	545	1075	500
34	2040	540	1075	510
35	1965	540	1020	500
36	2015	545	1065	500
37	2000	540	1065	500
38	1995	535	1050	500
39	2000	540	1070	500
40	2030	540	1080	500
41	2030	540	1075	500
42	1990	540	1065	500
43	2000	540	1090	505
44	1985	540	1030	505
45	2010	90	1055	90

TABLE XII

CYCLE FIRING PULSE

Test No. 9

Cycle	Firing Pulse Sec.	Cycle	Firing Pulse Sec.	Cycle	Firing Pulse Sec.
1	7.6	21	-	41	5.9
2	8.4	22	5.1	42	5.2
3	6.5	23	6.5	43	5.5
4	8.0	24	6.3	44	5.7
5	6.1	25	6.8	45	5.4
6	6.4	26	6.2	46	5.4
7	-	27	-	47	5.2
8	6.0	28	7.0	48	-
9	6.1	29	6.8	49	6.0
10	6.6	30	4.8	50	5.4
11	7.6	31	6.4	51	5.5
12	6.5	32	5.3	52	5.4
13	6.9	33	5.4	53	5.5
14	7.6	34	5.8		
15	7.0	35	6.9		
16	6.0	36	6.6		
17	6.6	37	6.3		
18	6.0	38	5.6		
19	-	39	6.1		
20	7.3	40	5.3		

TABLE XIII

MAXIMUM AND MINIMUM TEMPERATURE PER CYCLE

Test No. 9

Thermocouple T2

CYCLE	MAX.	MIN.	CYCLE	MAX.	MIN.	CYCLE	MAX.	MIN.
0	860	780						
1	1410	800	21	1250	830	41	1410	790
2	1460	805	22	1390	810	42	1380	800
3	1425	790	23	1415	805	43	1400	780
4	1480	800	24	1410	815	44	1420	800
5	1470	805	25	1425	825	45	1405	800
6	1450	850	26	1405	800	46	1420	835
7	1440	805	27	1750		47	1420	805
8	1420	800	28	1400	800	48	1410	800
9	1440	800	29	1450	805	49	1430	800
10	1420	790	30	1405	800	50	1415	860
11	1445	800	31	1415	790	51	1420	800
12	1430	800	32	1410	805	52	1430	805
13	1425	790	33	1390	780	53	1410	Amb.
14	1415	800	34	1400	780			
15	1405	790	35	1410	800			
16	1405	800	36	1430	785			
17	1430	800	37	1405	780			
18	1420	800	38	1400	790			
19	1420	805	39	1385	780			
20	1420	820	40	1390	790			

ARDÉ, INC.

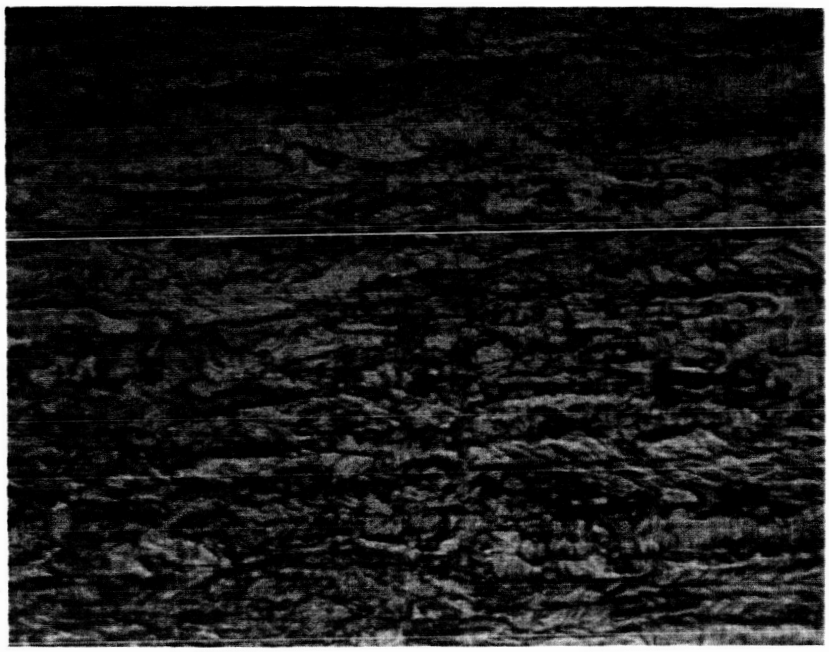

MURAKAMI'S ETCH 500X

MICROSTRUCTURE OF TUNGSTEN AS CONVENTIONALLY CONSOLIDATED BY PRESSING, SINTERING AND SWAGING

FIGURE 1

ARDÉ, INC.

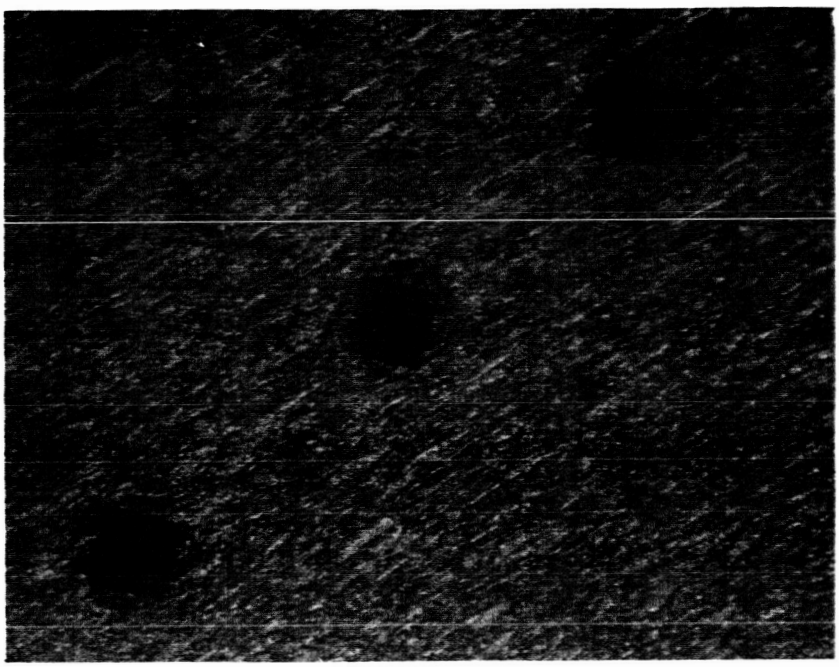

MURAKAMI'S ETCH 100X

MICROSTRUCTURE OF UNRECRYSTALLIZED TUNGSTEN
SHOWING VICKERS HARDNESS INDENTATIONS

FIGURE 2

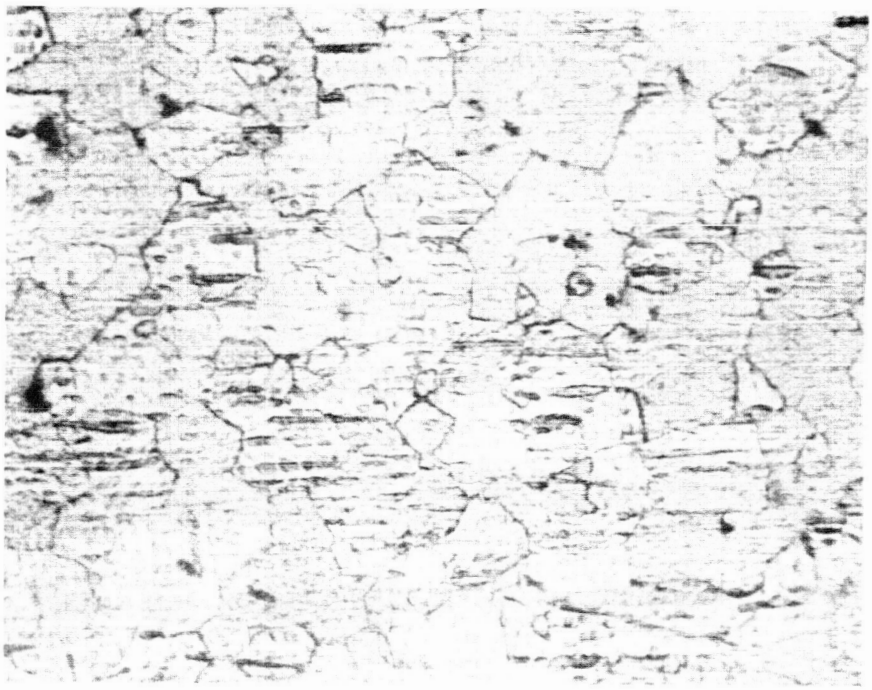

MURAKAMI's ETCH 500 X

MICRO STRUCTURE OF RECRYSTALLIZED

TUNGSTEN SAMPLE

FIGURE 3

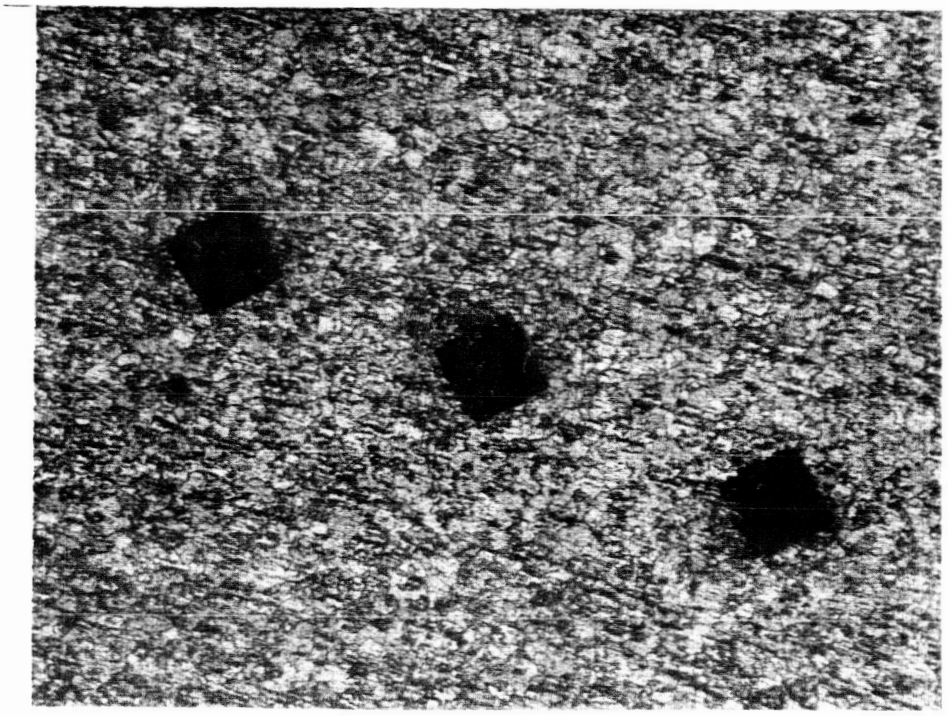

MURAKAMI'S ETCH 100 X

VICKERS HARDNESS INDENTATIONS
SHOWN IN RECRYSTALLIZED TUNGSTEN
MICRO STRUCTURE

FIGURE 4

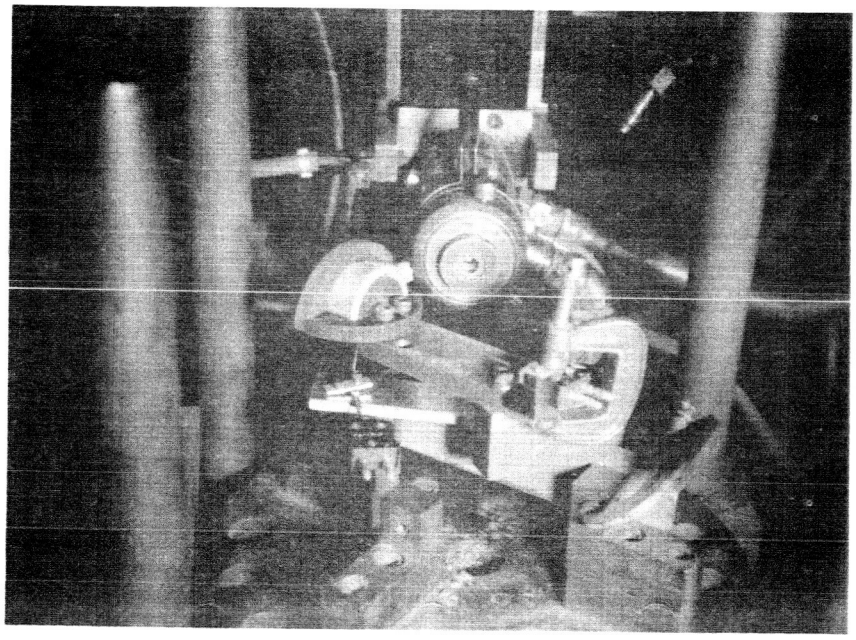

TEST SET-UP WITH SAMPLE OUT OF FIRING POSITION

FIGURE 5

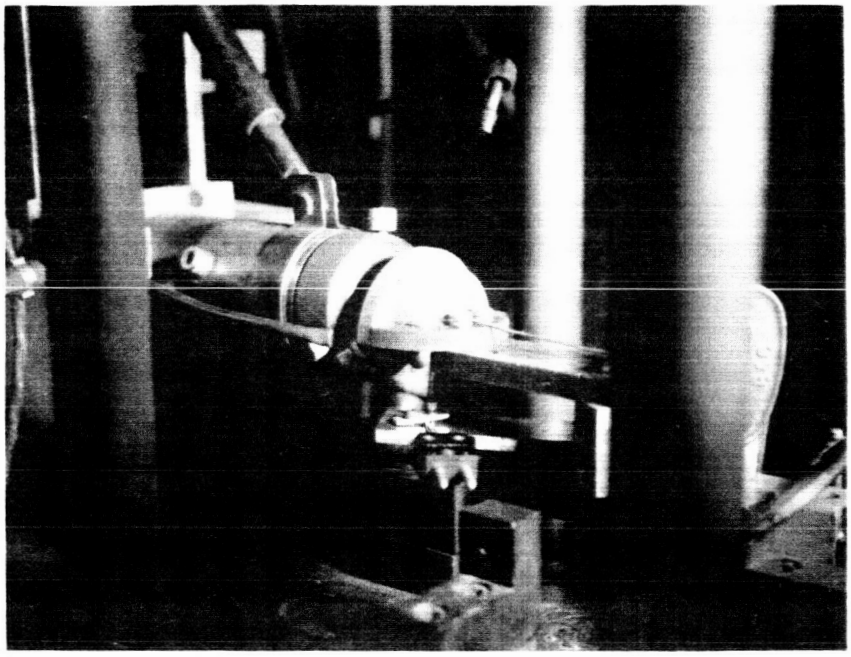

SAMPLE AND PLASMA TORCH IN FIRING POSITION

FIGURE 6

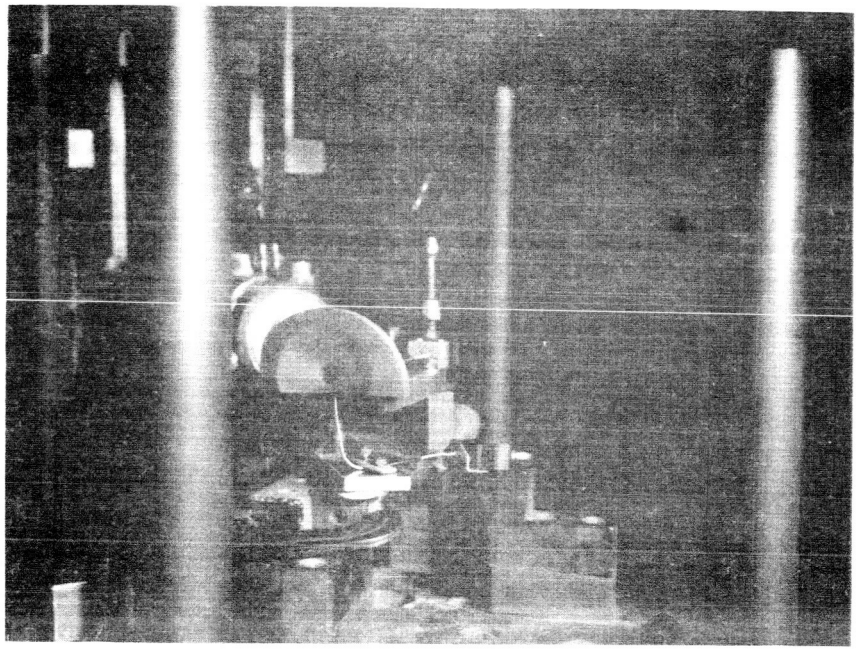

VIEW OF SAMPLE FRONT FACE
WITH PYROLYTIC GRAPHITE HEAT SHIELD
EXPOSING SAMPLE TARGET AREA

FIGURE 7

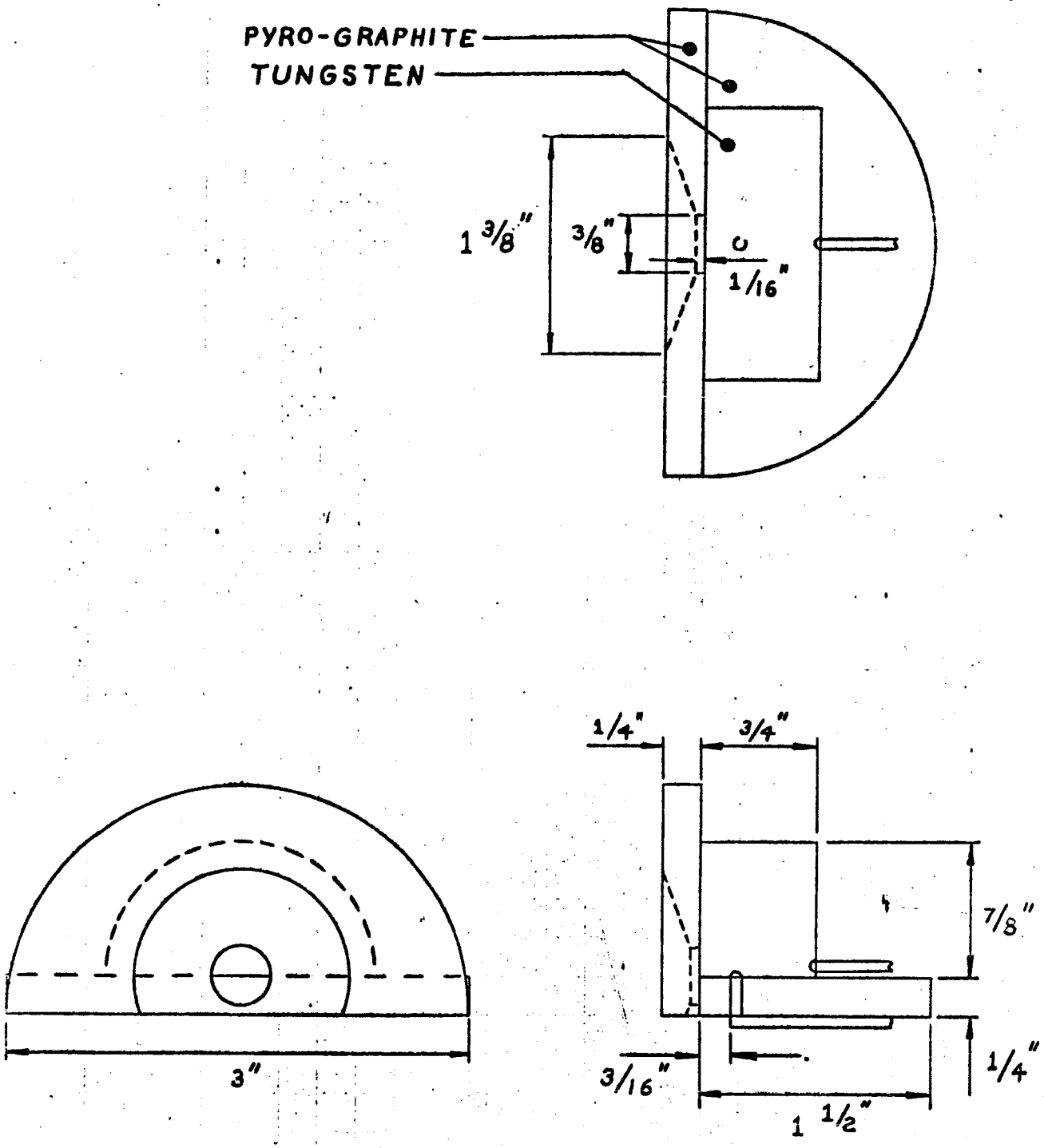

FIGURE 8 - PRELIMINARY TEST SET-UP

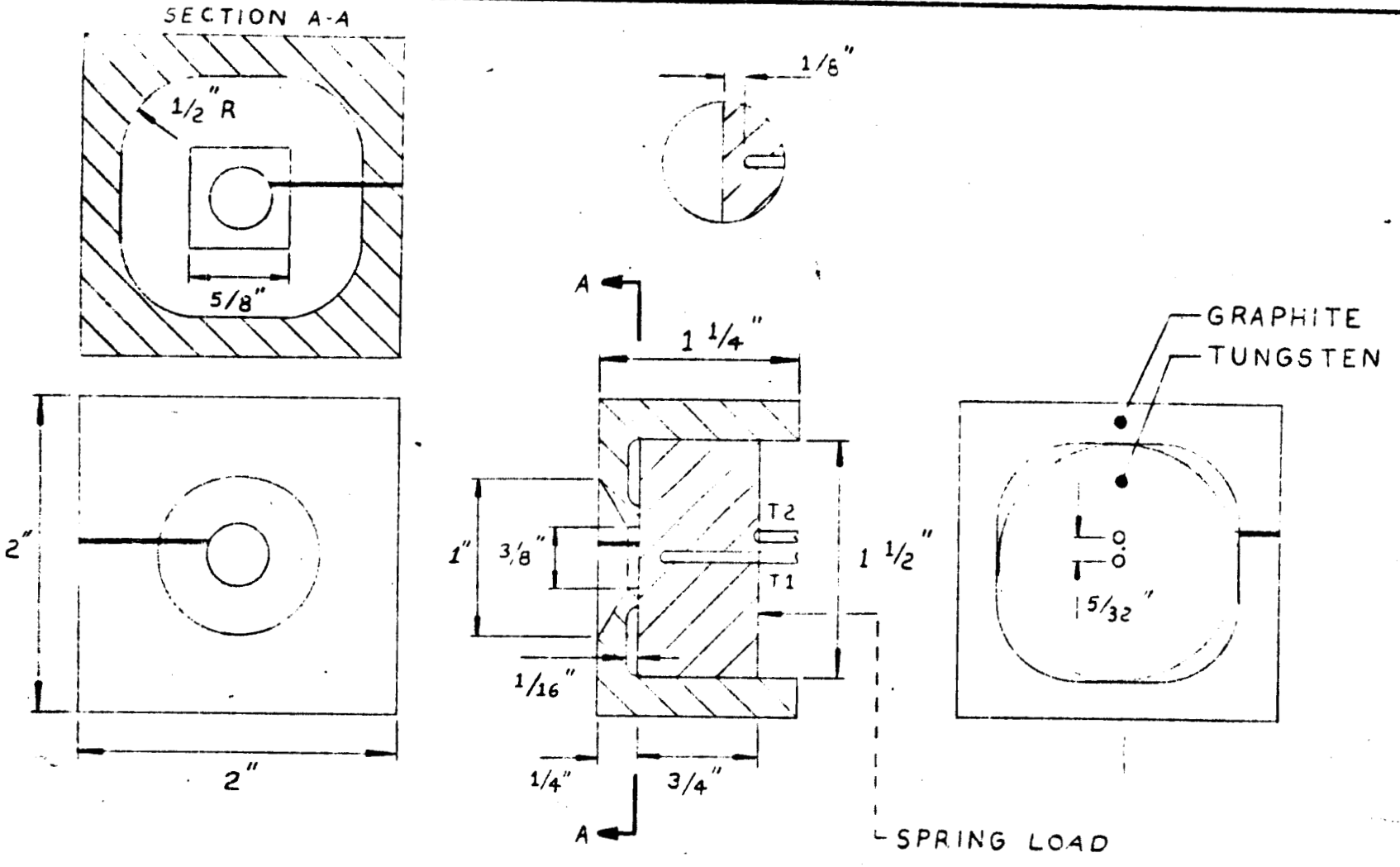

FIGURE 9 - GRAPHITE HOLDING BOX

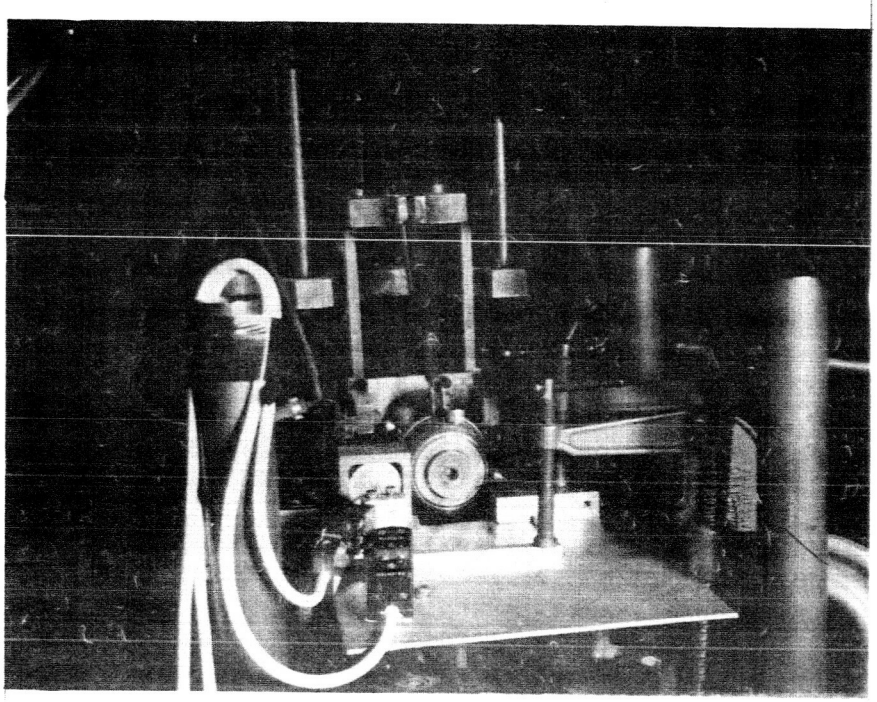

TEST SET-UP

FIGURE 10

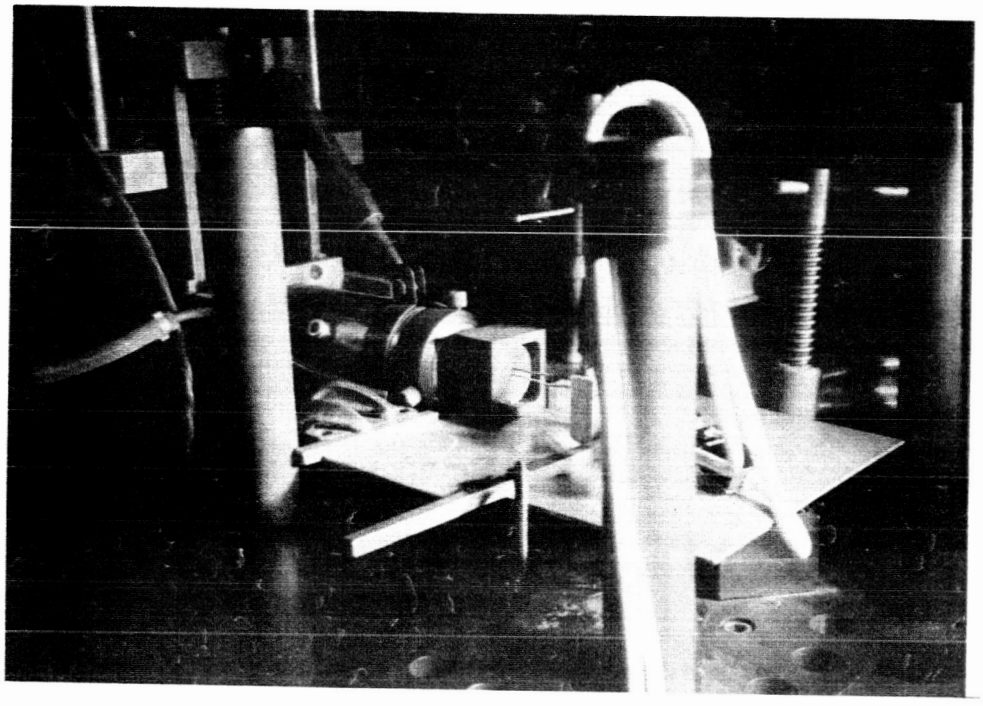

TEST SET-UP IN FIRING POSITION

FIGURE 11

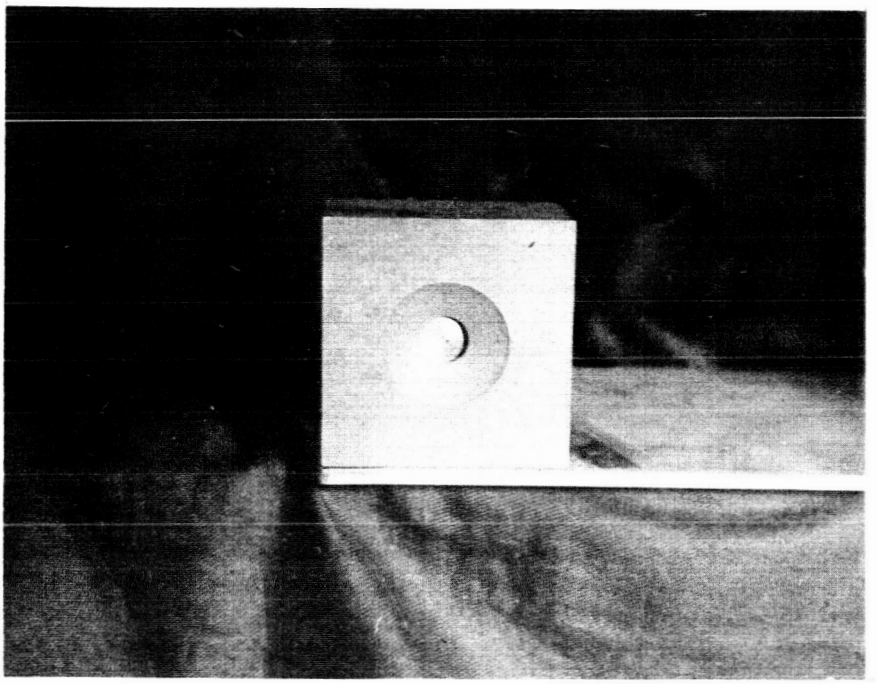

FRONT FACE OF SAMPLE SHOWING NEW HEAT SHIELD

AND EXPOSED SAMPLE TARGET AREA

BEFORE FIRING

FIGURE 12

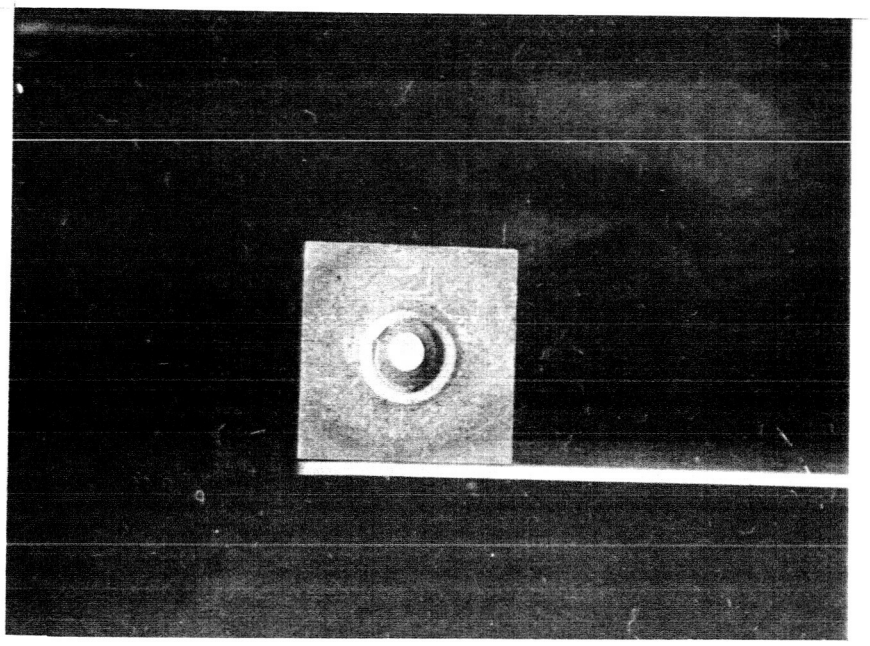

FRONT FACE OF SAMPLE SHOWING NEW HEAT SHIELD
AND EXPOSED SAMPLE TARGET AREA
AFTER FIRING

FIGURE 13

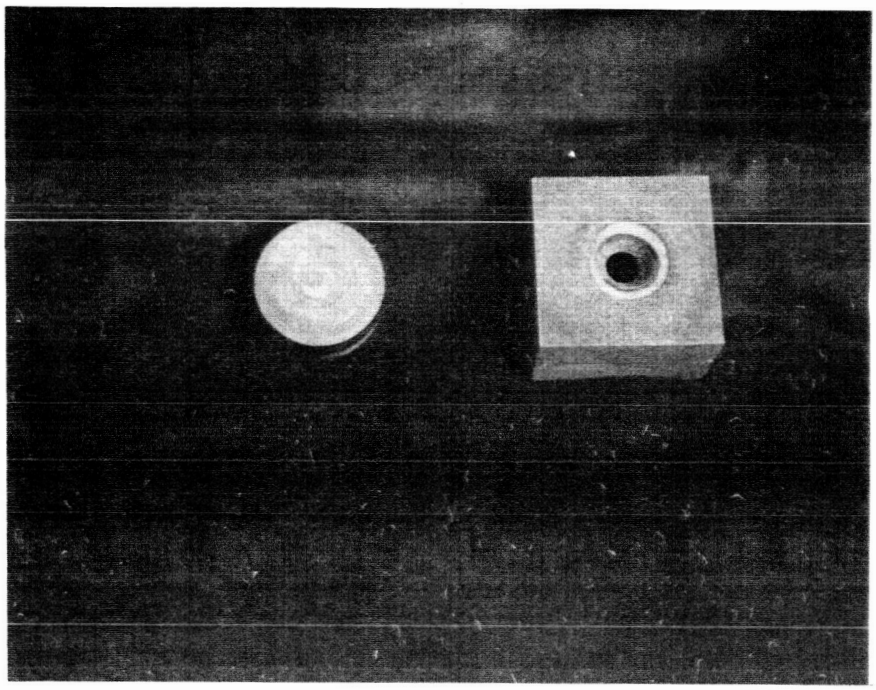

EXPLODED VIEW OF SAMPLE AND HEAT SHIELD

AFTER FIRING

FIGURE 14

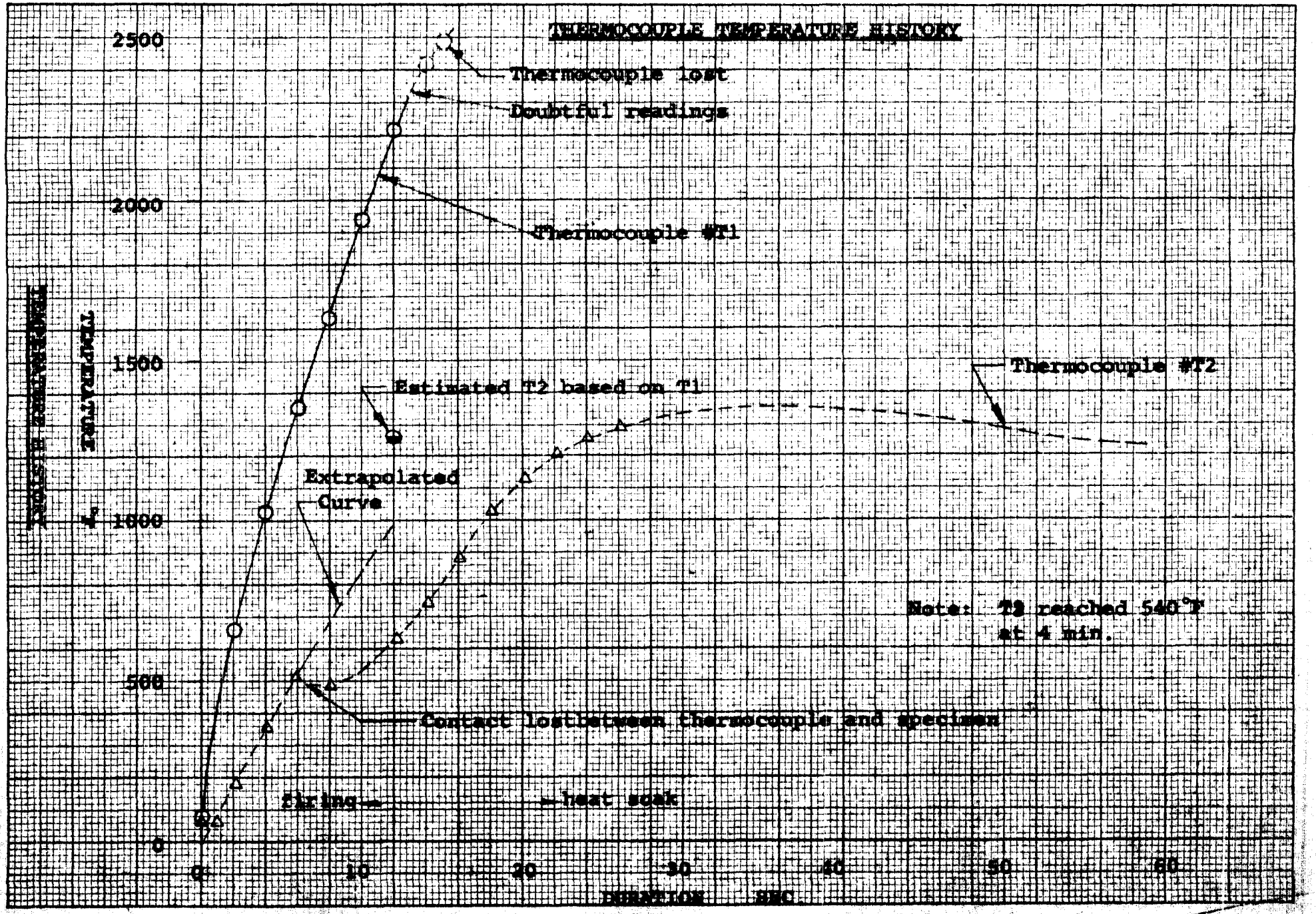

FIGURE 15

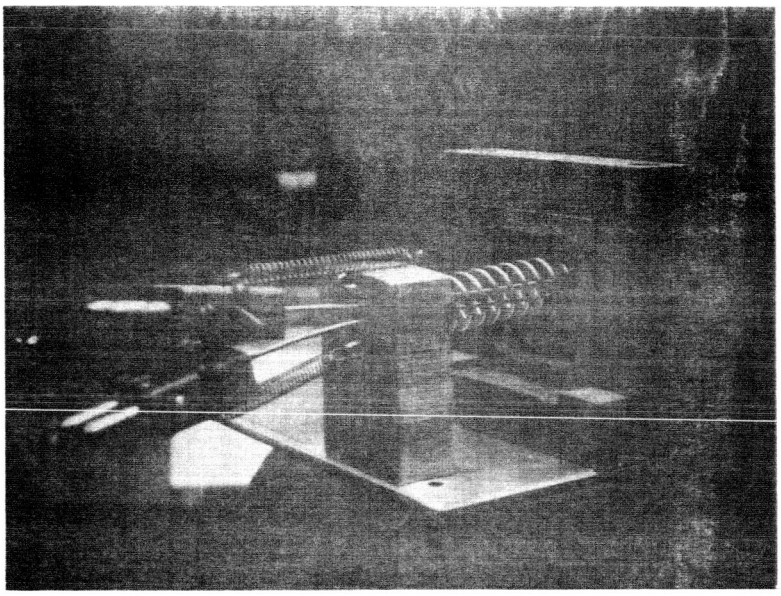

(a)

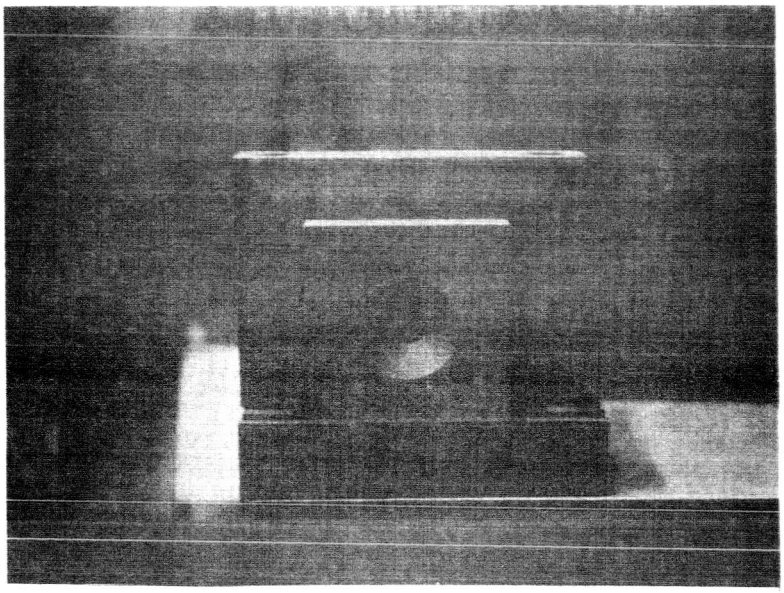

(b)

- SPRING LOADED TEST SETUP

FIGURE 16

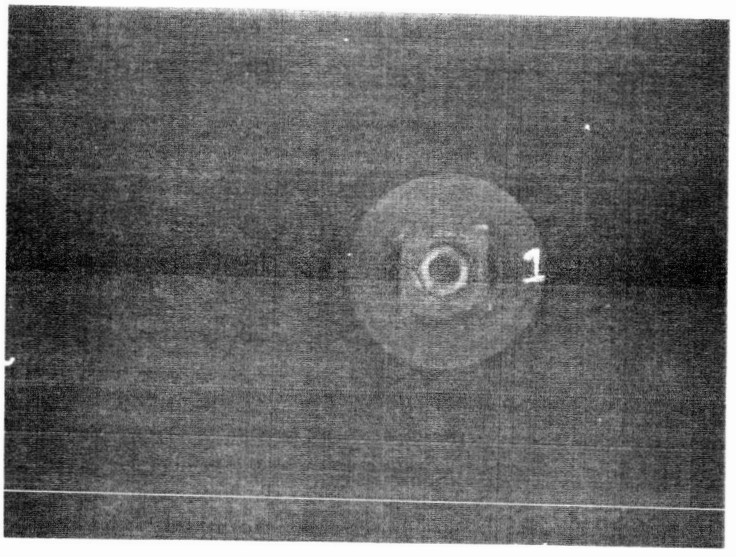

a) SAMPLE NO. 1 (with Argon cooling)

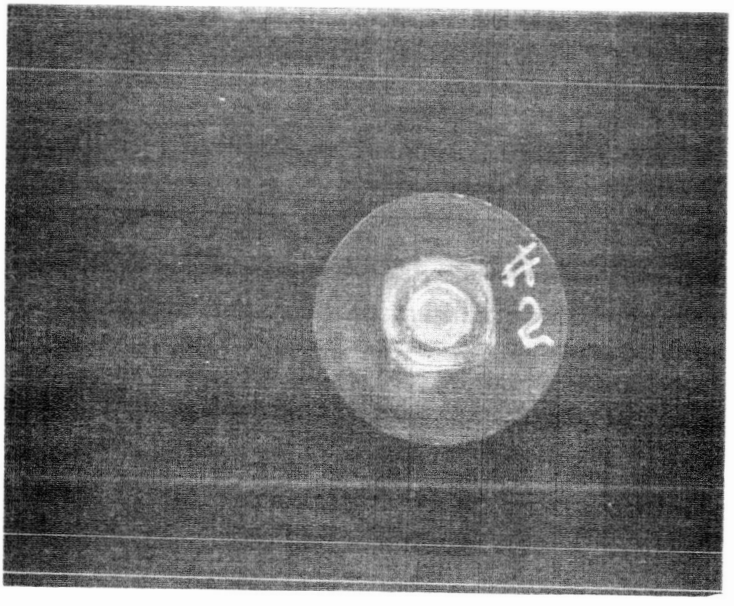

b) SAMPLE NO. 2 (no cooling)

- POST-FIRED RECRYSTALLIZED SAMPLES

FIGURE 17

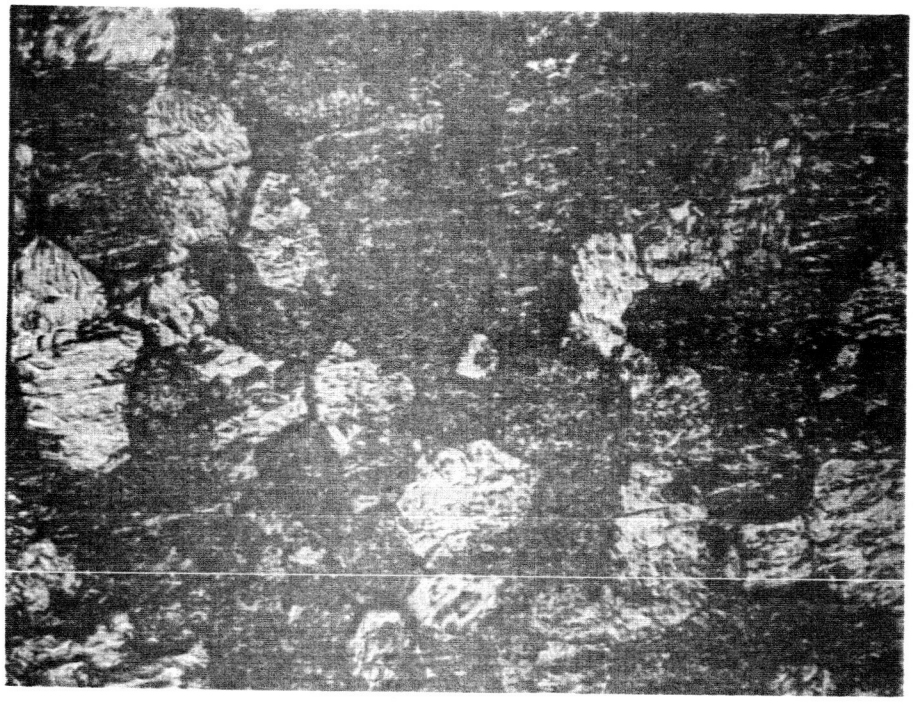

MURAKAMI's ETCH 500 X

a) MICROSTRUCTURE

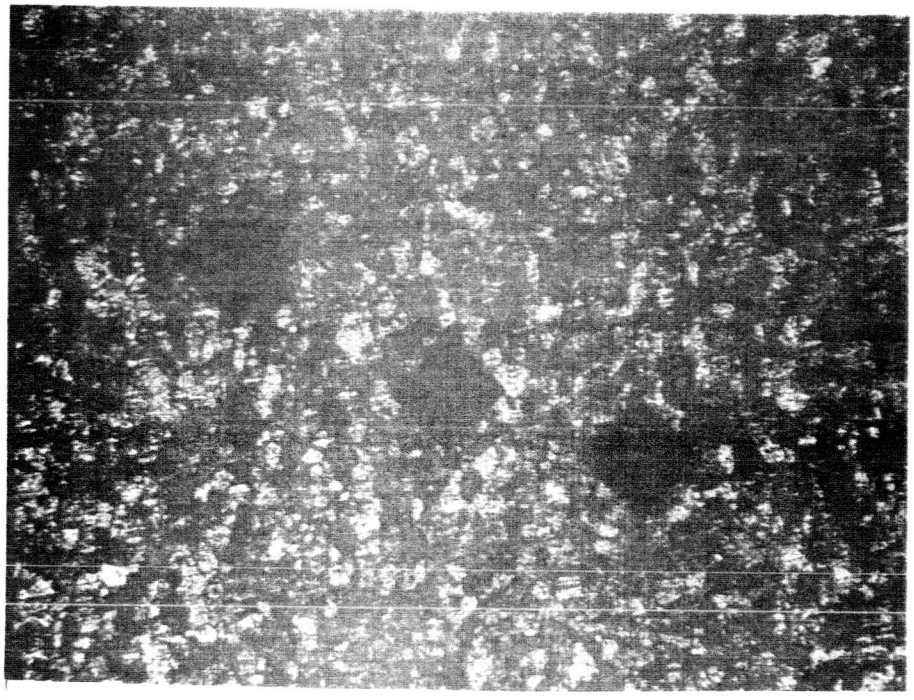

MURAKAMI'S ETCH 100 X

b) VICKERS HARDNESS INDENTATIONS

- MICROSTRUCTURES OF RECRYSTALLIZED SAMPLE NO. 1

FIGURE 19

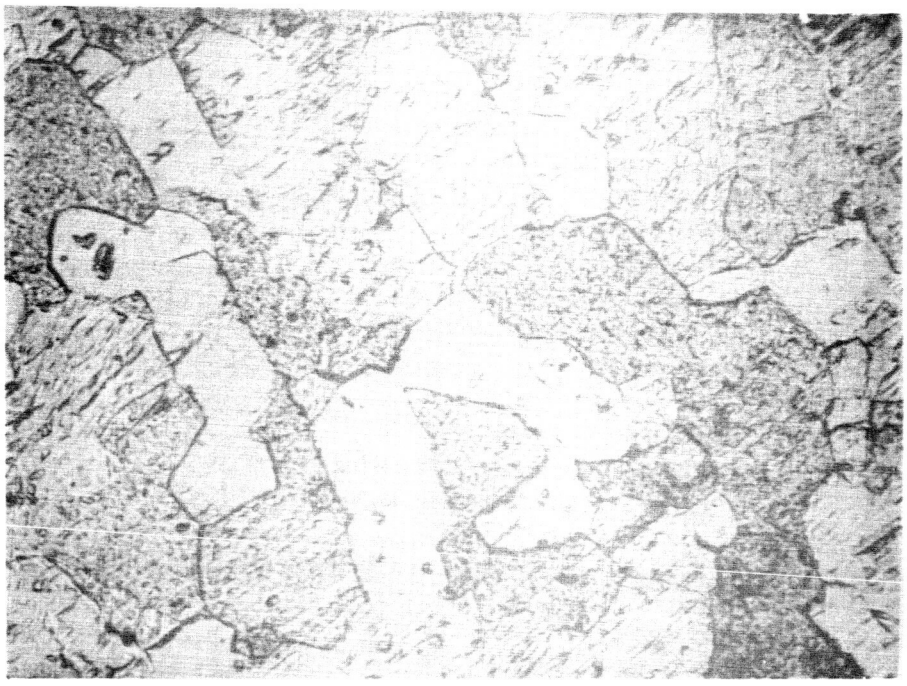

MURAKAMI'S ETCH 500 X

a) MICROSTRUCTURE

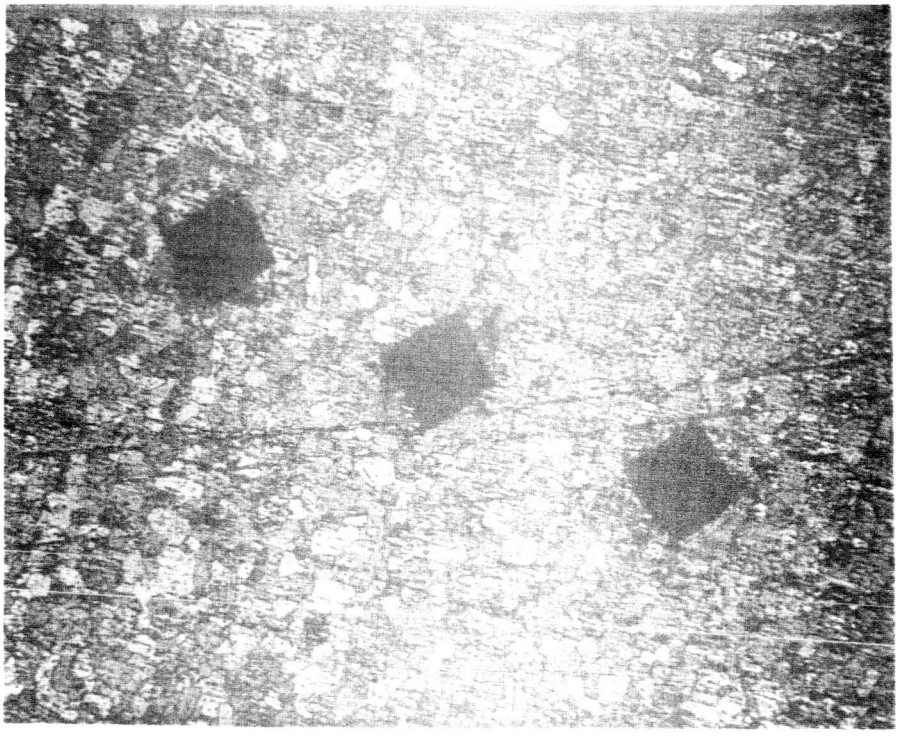

MURAKAMI'S ETCH 100 X

b) VICKERS HARDNESS INDENTATIONS

- MICROSTRUCTURES OF RECRYSTALLIZED SAMPLE NO. 2

FIGURE 19

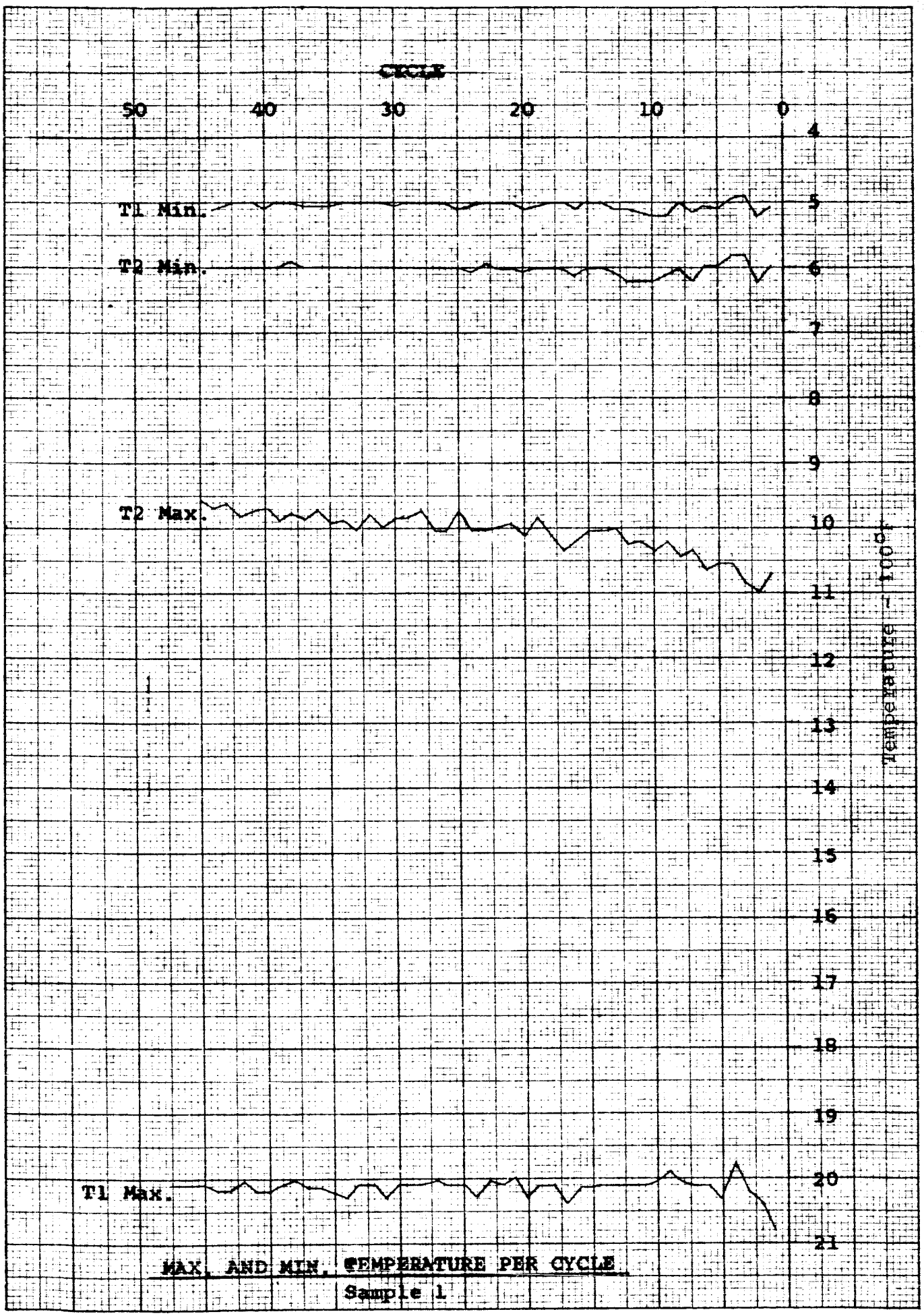
CYCLE
50
40
30
20
10
0
T1 Min.
T2 Min.
T2 Max.
T1 Max.
Temperature - 100+
4
5
6
7
8
9
10
11
12
13
14
15
16
17
18
19
20
21
MAX. AND MIN. TEMPERATURE PER CYCLE
Sample 1

Figure 20

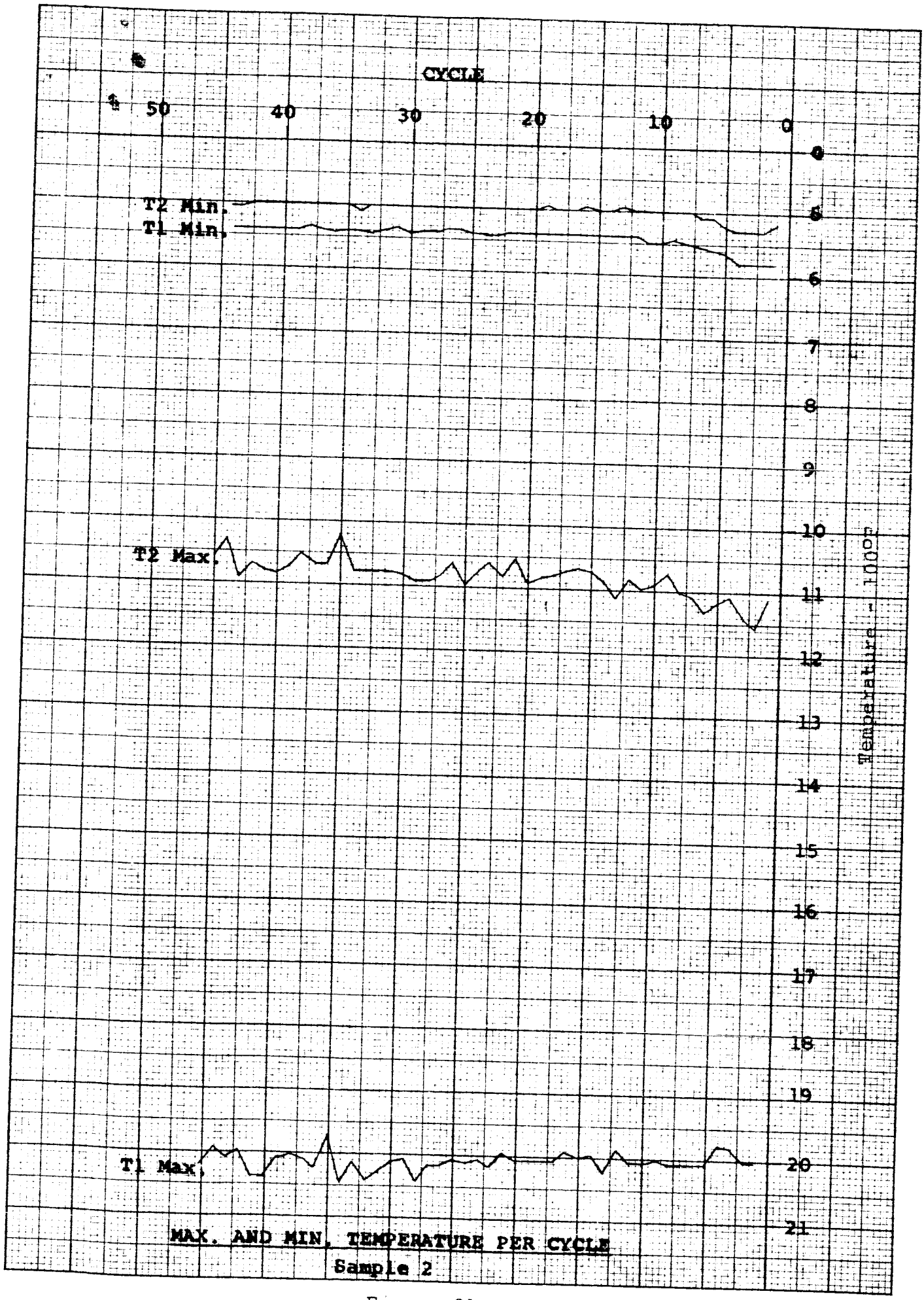
CYCLE
50
40
30
20
10
0
T2 Min.
T1 Min.
T2 Max.
T1 Max.
Temperature - 100°F
MAX. AND MIN. TEMPERATURE PER CYCLE
Sample 2

Figure 21

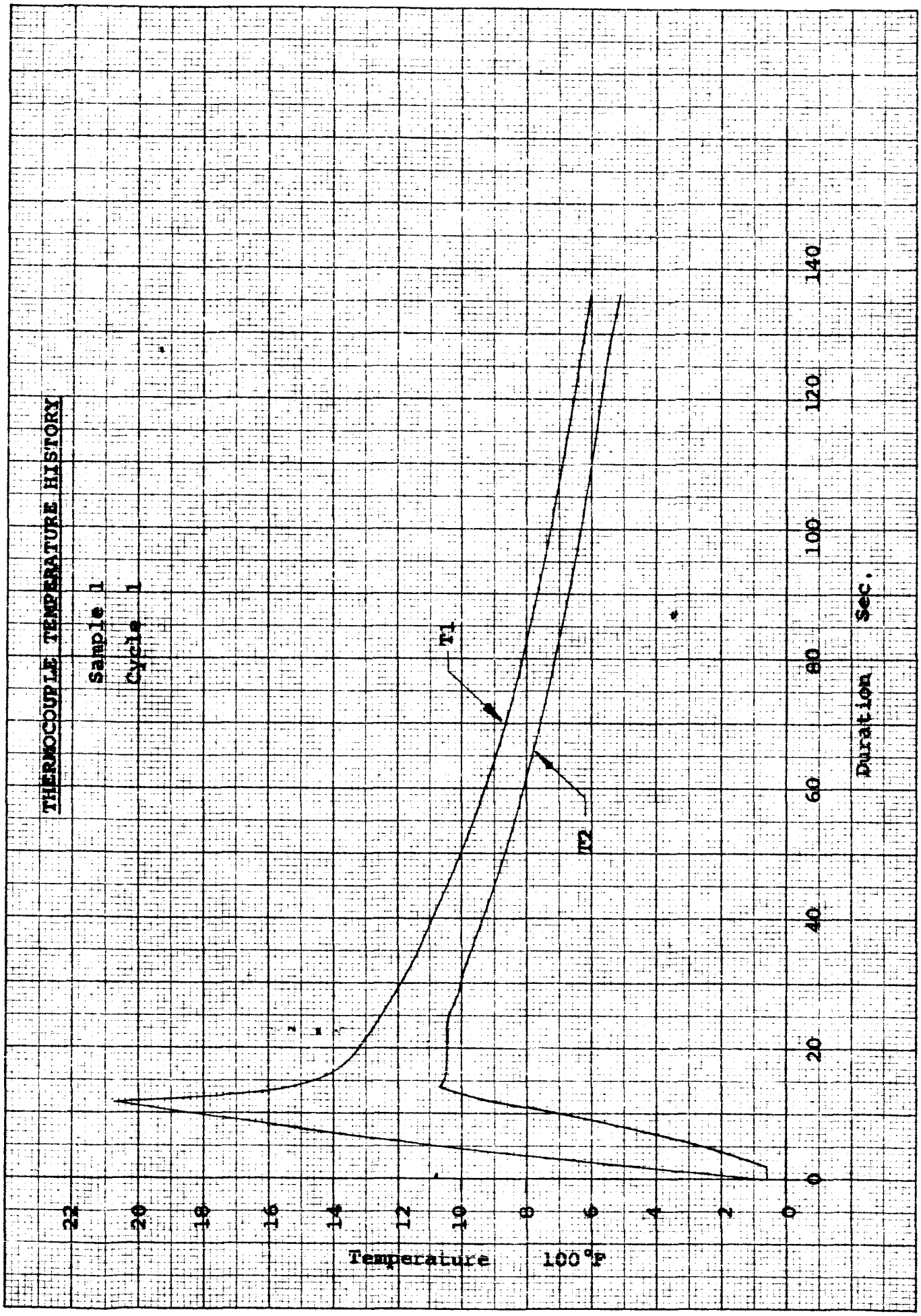
THERMOCOUPLE TEMPERATURE HISTORY
Sample 1
Cycle 1
T1
T2
Temperature 100°F
Duration Sec.
0
2
4
6
8
10
12
14
16
18
20
22
0
20
40
60
80
100
120
140

Figure 22

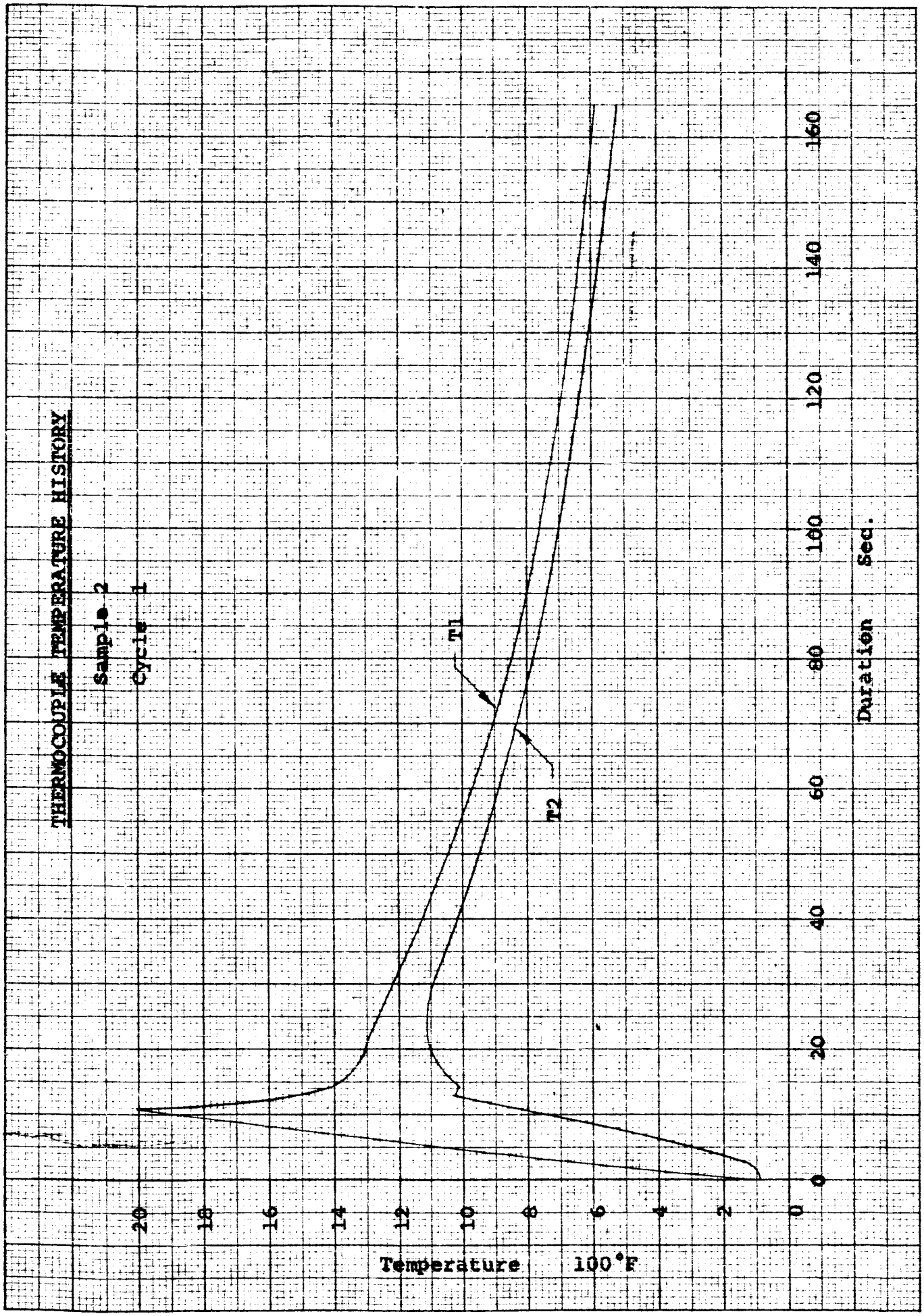
THERMOCOUPLE TEMPERATURE HISTORY
Sample 2
Cycle 1
T1
T2
Temperature 100°F
Duration Sec.
0
2
4
6
8
10
12
14
16
18
20
0
20
40
60
80
100
120
140
160

Figure 23

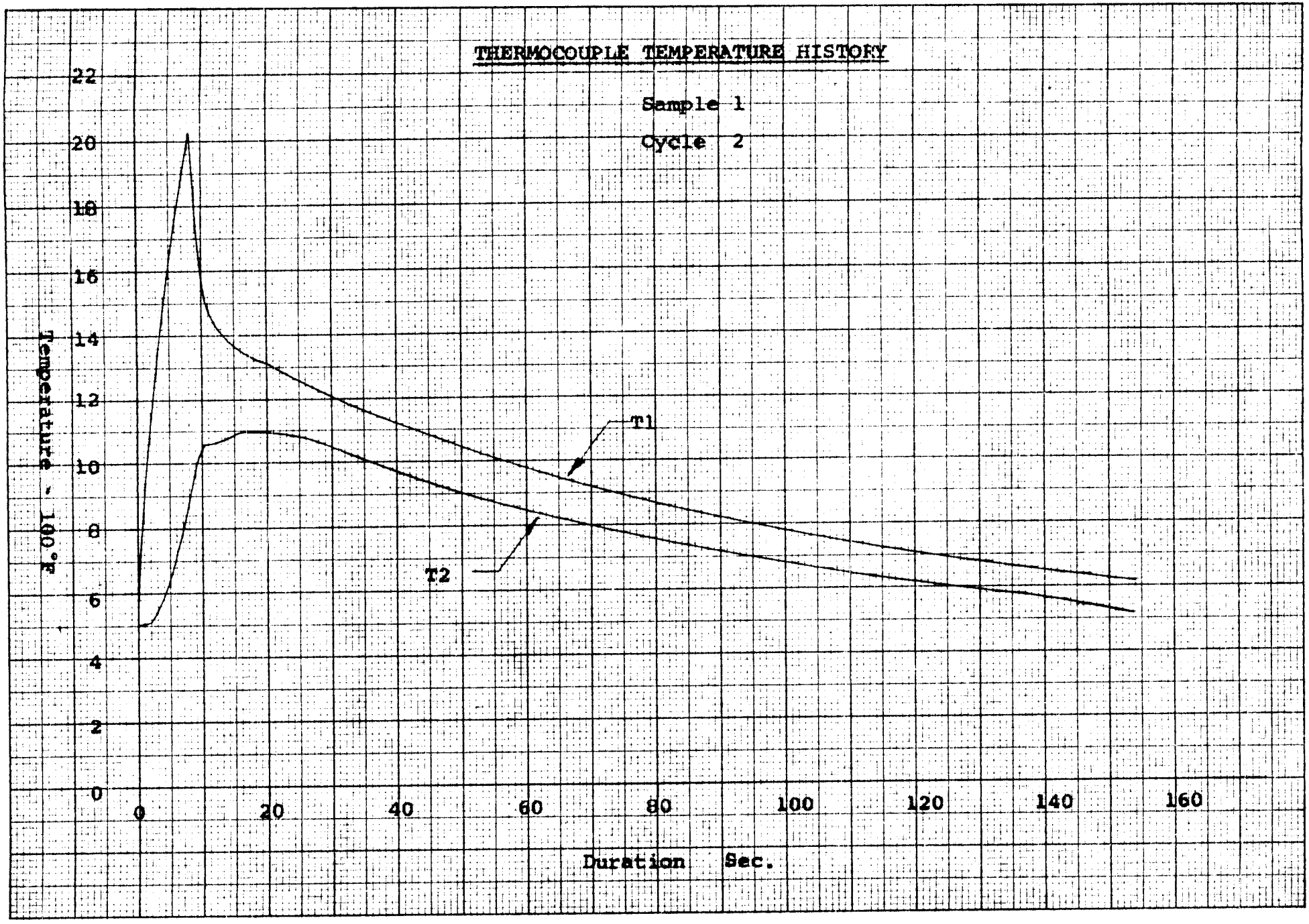

Figure 24

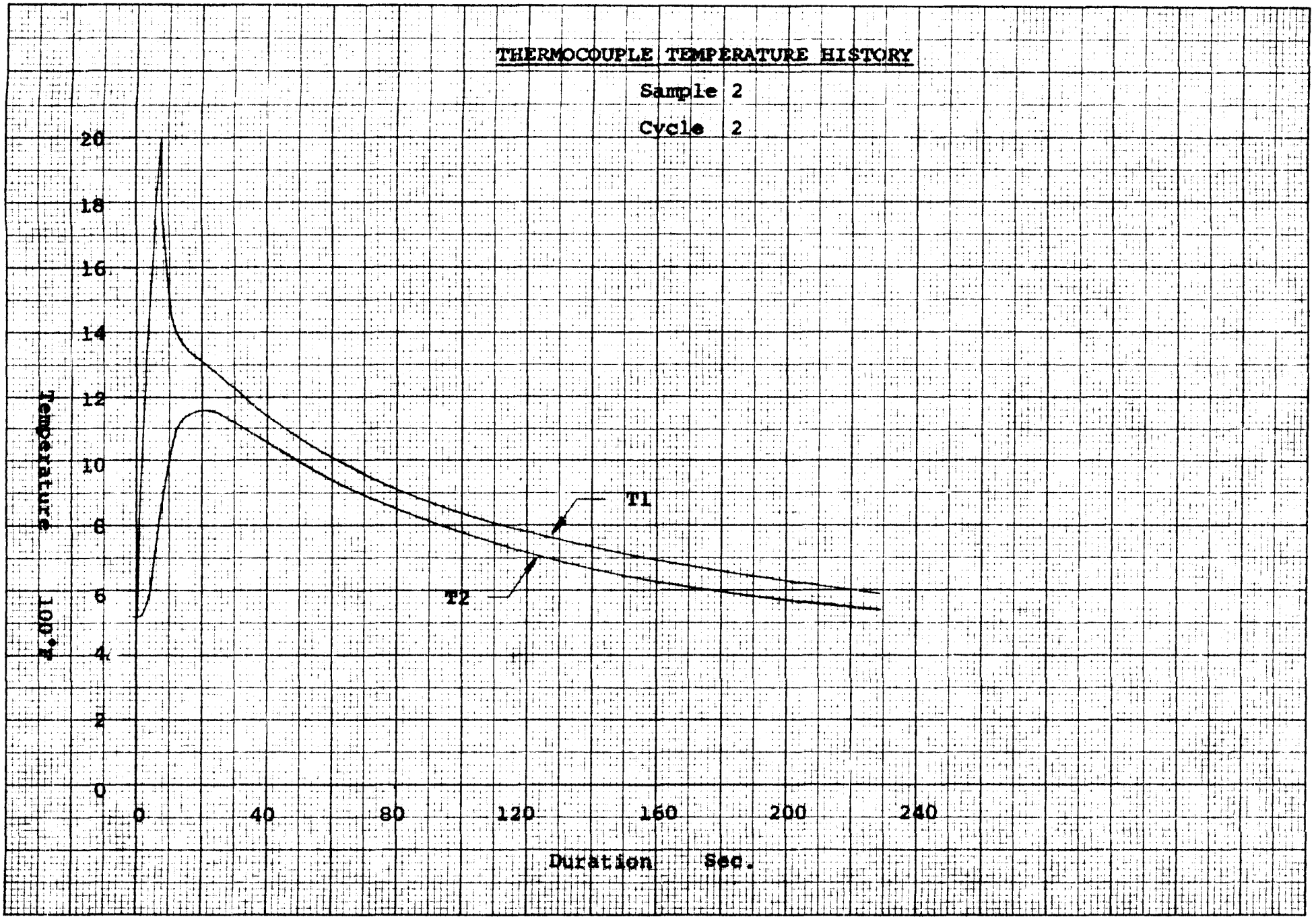

Figure 25

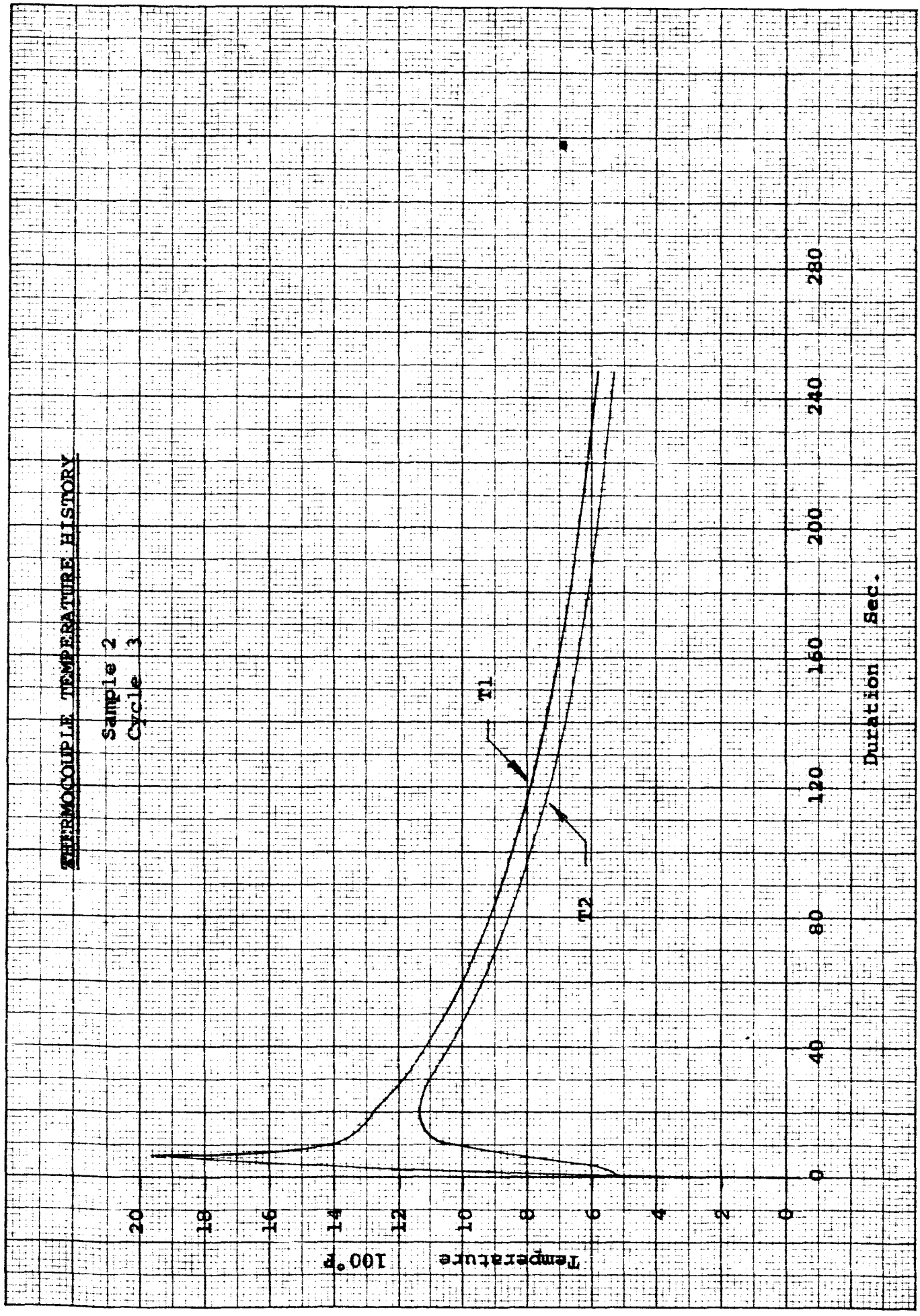

Figure 26

THEORETICAL STRAIN AND CYCLING CHARACTERISTICS

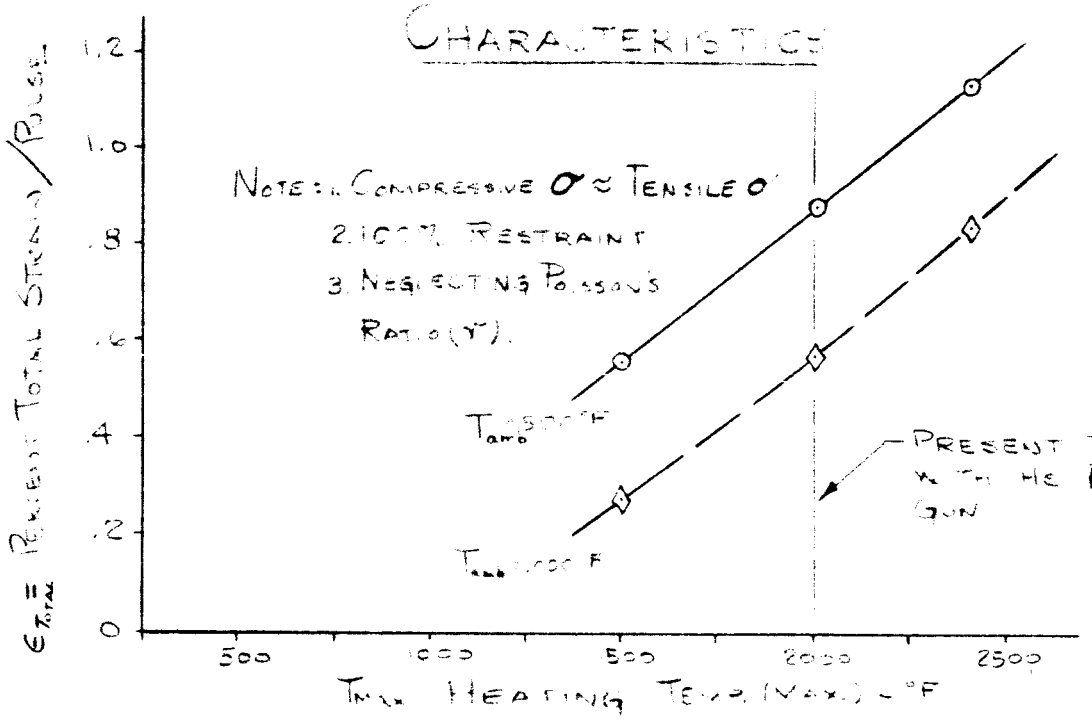

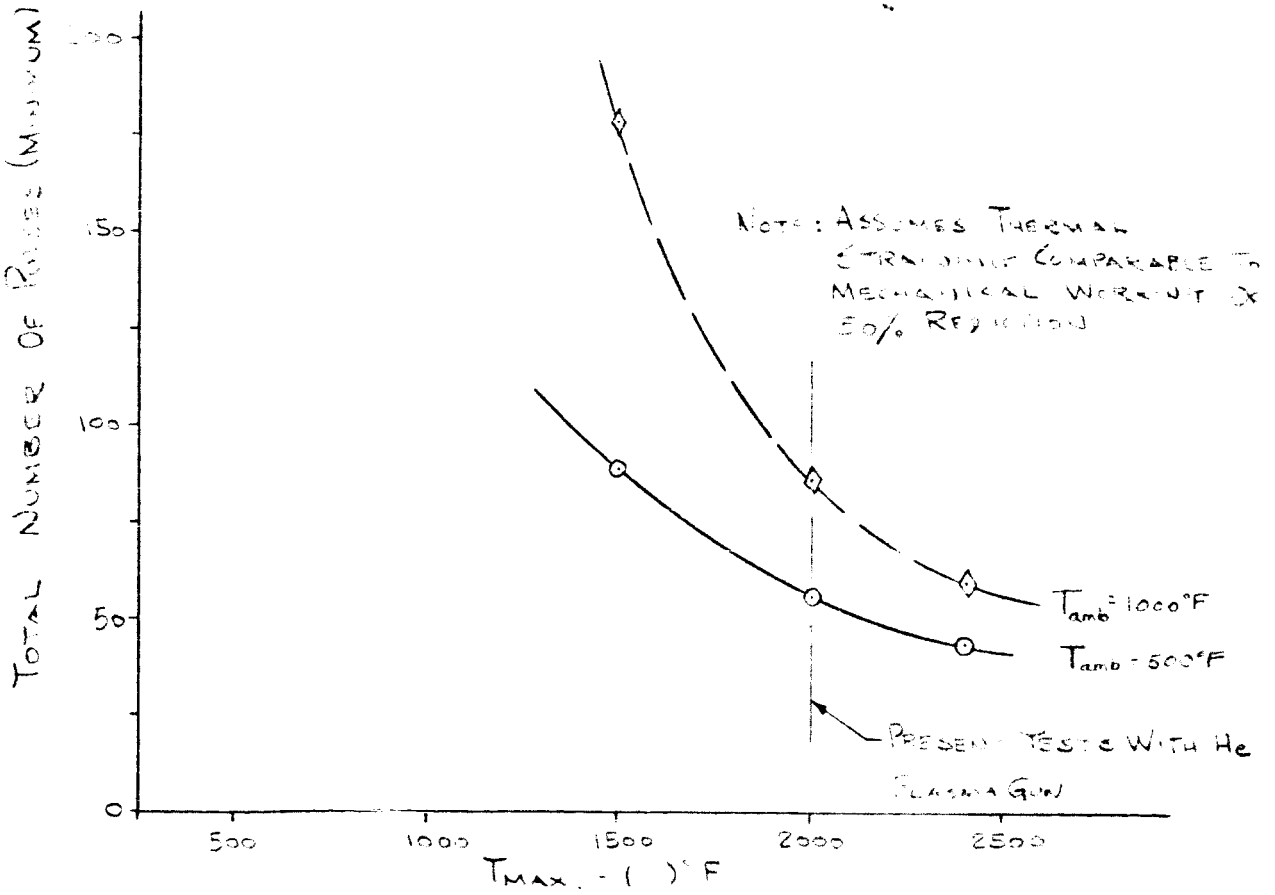

FIG. 27

Stress-Strain Characteristics of Recrystallized Tungsten[F]

Notes: From NMIC Report 127
F- 1 hour @ 2900°F

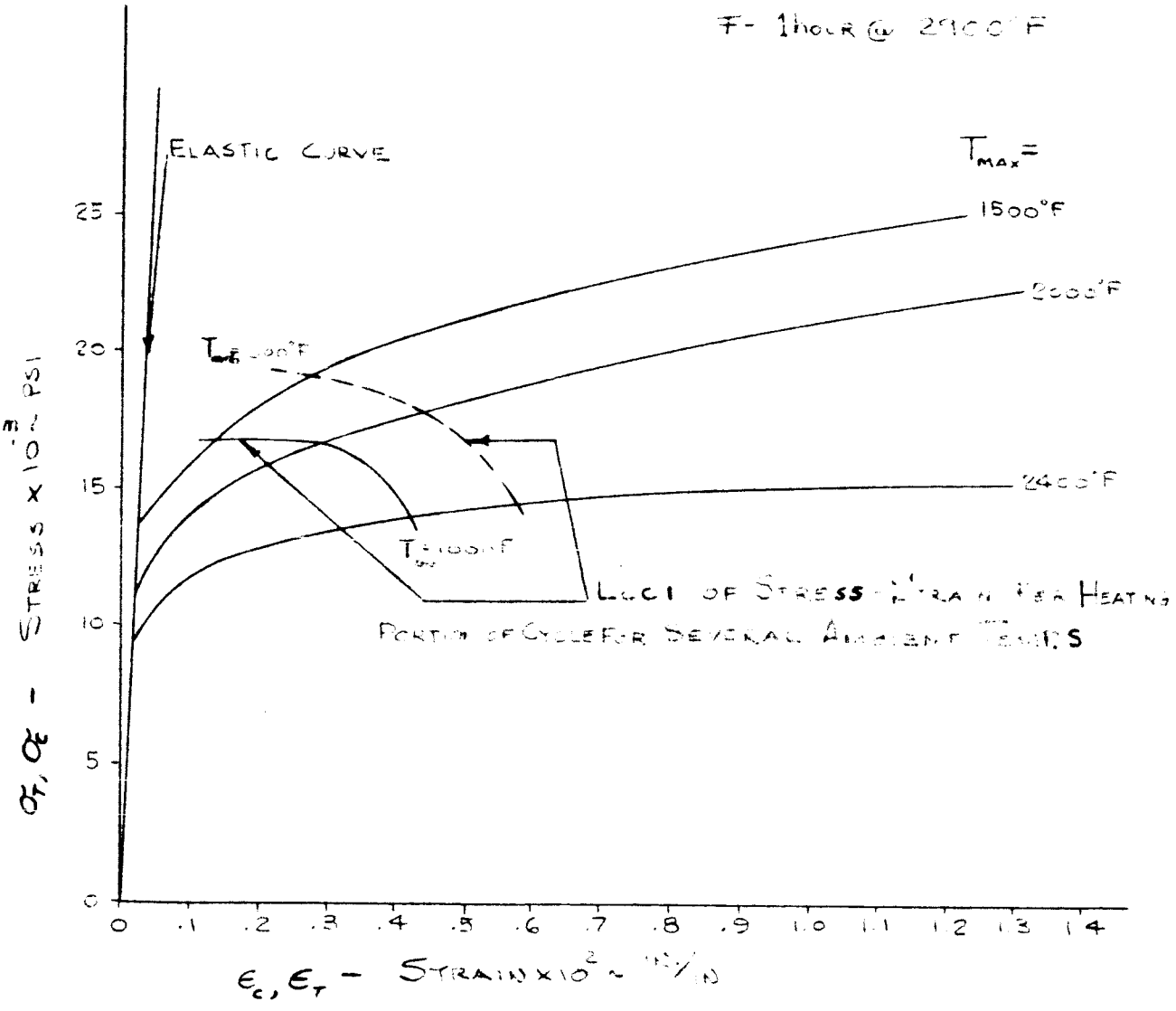

Fig 28

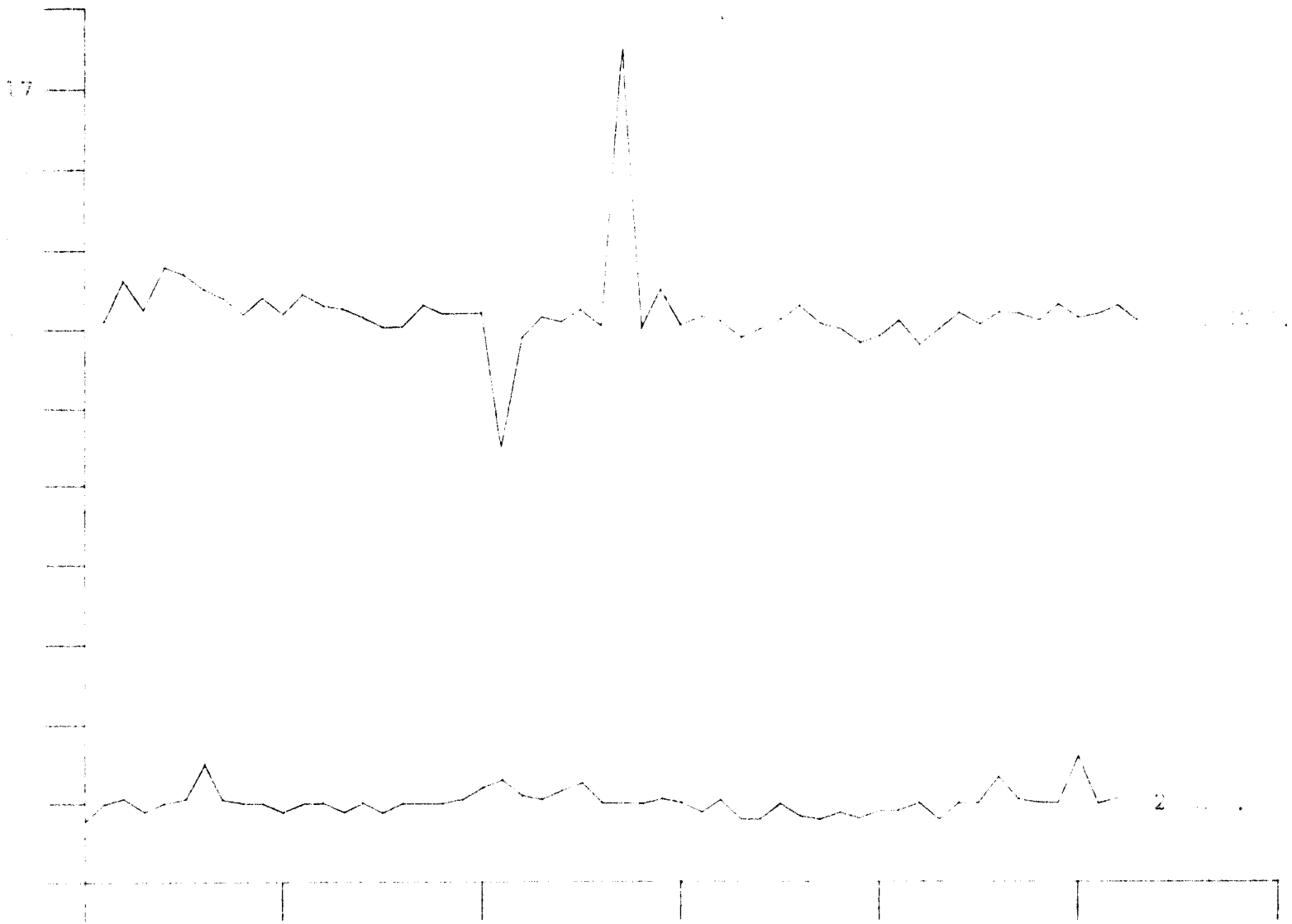
17
2